

Risk Analysis of Equity-Bond Portfolios with Default-Driven Stock Price Jumps



UNIVERSITY OF GOTHENBURG
SCHOOL OF BUSINESS, ECONOMICS AND LAW

Emil Sturesson, Anton Wennström

Supervisor: Alexander Herbertsson

Graduate School, School of Business, Economics and Law

University of Gothenburg, Sweden

Master's Thesis in Finance, Spring Term 2025

Abstract

In this thesis, we study the risk of a portfolio consisting of stocks and bonds, where bond defaults trigger downward jumps in stock prices. To evaluate the portfolio's risk exposure, we use Value-at-Risk (VaR) as the primary risk measure. The analysis focuses on a portfolio where the stocks are assumed to be large and homogeneous, and the bond holdings may include any number of defaultable bonds, provided they are exchangeable. The modeling framework is based on the stock-bond setup introduced by Herbertsson (2025b), which explicitly incorporates equity price jumps at bond default events. We extend this framework by analyzing a range of portfolio configurations and testing sensitivity to different asset correlation structures. Default probabilities are estimated using the saddlepoint approximation derived in Herbertsson (2023). To model dependence between bond defaults, we apply both the one-factor Gaussian copula and the Clayton copula, offering flexibility in capturing joint default behavior. Our results show that a stock-bond portfolio with stocks following the model in Herbertsson (2025b) yields substantially higher VaR estimates compared to the case where stocks follow the classical Black and Scholes (1973) model. We also demonstrate that VaR is highly sensitive to the choice of copula parameters, and that increasing the portfolio's stock allocation generally results in higher risk levels.

Acknowledgment

We would like to express our sincere gratitude to our supervisor, Professor Alexander Herbertson, for his valuable guidance and continuous support throughout the course of this thesis. His insightful feedback, clear direction, and deep expertise in the field have been instrumental in shaping the research and improving its quality. We are particularly grateful for the time and guidance he provided, which contributed meaningfully to the academic depth of this thesis.

Contents

1	Introduction	4
2	Literature Review	5
2.1	Jump Models	6
2.2	Credit Risk Modeling	8
2.3	Value-at-Risk	9
3	Methodology	10
3.1	Herbertsson's Model	11
3.1.1	Modelling Stock Prices	12
3.1.2	Modelling Bond Prices	15
3.1.3	Portfolio Loss Process	16
3.1.4	Value-at-Risk	18
3.2	Saddlepoint Approximation for the Distribution of Defaults	20
3.3	Copulas	22
3.3.1	One-factor Gaussian Copula	22
3.3.2	Clayton Copula	23
4	Results	25
4.1	Default Distribution	25
4.1.1	Default Distribution under the One-Factor Gaussian Copula	25
4.1.2	Default Distribution under the Clayton copula	28
4.2	Value at Risk	30
4.2.1	Value at Risk Estimation Using the One-Factor Gaussian Copula	31
4.2.2	Value at Risk Estimation Using the Clayton Copula	37
5	Conclusion	44

1 Introduction

Financial markets are subject to multiple sources of risk, particularly from equity price fluctuations and credit events such as corporate defaults. While traditional risk models often assume that asset prices evolve continuously over time, real-world financial markets frequently experience sudden, sharp movements triggered by unexpected events, including financial crises, credit downgrades, and large-scale defaults. These abrupt shocks introduce discontinuities that challenge conventional risk modeling and portfolio management techniques.

Historical examples highlight the need for models that capture these discontinuities. For example, the 2008 global financial crisis triggered a cascade of defaults in the subprime mortgage market and led to severe losses across equity and credit markets, see Guerrero et al. (2008) and Johnson and Mamun (2012). More recently, the COVID-19 pandemic caused extreme market volatility and widespread credit downgrades. Regional events, such as the 2011 European sovereign debt crisis and the collapse of Evergrande in China, have also sent shockwaves through financial markets. These cases underscore the need for risk models capable of capturing sudden, discontinuous shifts in asset prices.

To address the challenge of capturing the discontinuous dynamics of asset prices following default events for large firms or sovereign states, this paper analyzes losses in a portfolio consisting of stocks and coupon-paying bonds. A key feature of our study is that each bond default not only results in a loss on the bond itself but also triggers an immediate downward jump in the stock prices. This creates a compounding negative effect, as defaults simultaneously impact both asset classes. Our analysis is based on the framework developed in Herbertsson (2025b), which extends the results of Herbertsson (2025a) by incorporating bonds into a previously stock-only portfolio. While Herbertsson (2025a) examines the effect of credit defaults on stock prices in a pure equity setting, Herbertsson (2025b) generalizes this to a mixed stock–bond portfolio. In our work, we further extend the analysis by exploring a broader range of portfolio configurations, focusing in particular on how different stock-bond allocations and asset correlations affect portfolio risk in the presence of sudden credit events. For parts of the numerical implementation, we draw on computational methods introduced in Herbertsson (2023). To model dependence between default times, we employ copula models, specifically the one-factor Gaussian and Clayton copulas, and use them to estimate portfolio risk through the Value-at-Risk (VaR) metric

which is simply the α -quantile of the portfolio loss, for some α in $(0, 1)$. We also compare these VaR estimates to those obtained under a classical Black-Scholes framework to highlight the importance of accounting for jump risk and default dependence in risk modeling.

Our results show that the choice of copula significantly affects the VaR, where the Clayton copula generally produces higher VaR estimates than the one-factor Gaussian copula, particularly at high confidence levels, making it more suitable for capturing tail events involving multiple simultaneous defaults. We also find that VaR increases as the portfolio becomes more stock-heavy, reflecting the greater exposure to market shocks. Additionally, for high levels of asset correlation, the VaR exhibits non-linear behaviors, including sharp jumps, especially at higher confidence levels, highlighting the sensitivity of risk to both allocation and dependence structure. In particular, we also see that $\text{VaR}_{95\%}$ and $\text{VaR}_{99\%}$ start to decrease as the correlations become very high. Finally, when comparing the relative difference in estimated VaR between the copula based framework to the classical Black-Scholes model, we find that it can exceed 1000%, even over short time horizons.

The remainder of this thesis is organized as follows. Section 2 reviews the existing literature that forms the foundation of this study, with a focus on key contributions in the areas of credit risk, default modeling, loss probabilities, and risk measures. In Section 3, we provide a detailed overview of the models employed in our analysis, with particular emphasis on the framework proposed by Herbertsson (2025b). This section also includes comprehensive explanations of the theoretical foundations and methodologies that underpin our results. Section 4 presents our empirical findings, highlighting VaR estimates across different modeling frameworks and parameter settings to assess the influence of various portfolio components. Finally, Section 5 offers concluding remarks and summarizes the main insights derived from the analysis.

2 Literature Review

In this section, we review the relevant literature on portfolio modeling under credit risk, with particular focus on models that incorporate jumps to capture the effects of sudden and discontinuous market events. Jump models form the theoretical foundation of this paper, providing a framework for describing the dynamics of portfolio value in the presence of sudden credit shocks, such as defaults. These models have been widely studied in various settings for both

stocks and bonds. However, as pointed out by Herbertsson (2025b), the literature has rarely addressed scenarios in which a portfolio simultaneously includes both asset classes and where stock prices exhibit downward jumps triggered by defaults of the bonds within the same portfolio. This represents a notable gap, as most asset managers oversee portfolios composed of both stocks and bonds. Therefore, incorporating both asset types into the analysis not only adds a layer of realism but also introduces dynamics between the assets that can significantly affect the portfolio, especially in the presence of jump risk.

In Subsection 2.1 we review key contributions to the development of jump-based models, with a focus on the various extensions that have been proposed to capture sudden changes in asset prices. Subsection 2.2 examines previous literature on credit risk modeling relevant to our study, highlighting influential work on default intensity models, loss distributions, and the use of risk measures in credit-sensitive settings. Finally, in Subsection 2.3, we review prior research on VaR, which is the risk measure applied in this thesis, and highlight key properties discussed in the existing literature.

2.1 Jump Models

Empirical evidence supports the presence of both continuous and jump components in asset prices, see among others Bates (2000), Chernov et al. (2003), and Eraker (2004). Merton (1976) extends the option pricing framework of Black and Scholes (1973) by allowing the underlying asset to follow a jump-diffusion process. In this framework, asset prices evolve according to a geometric Brownian motion (GBM), which models continuous paths driven by a deterministic drift and a stochastic diffusion term. A key feature of GBM is that the increments between any two time points are independent and normally distributed, with mean zero and variance proportional to the length of the time interval. This implies a smooth evolution of prices and normally distributed returns over short horizons. However, such a framework is unable to account for sudden and significant price movements that occur during periods of financial stress. To address this, Merton (1976) introduces a jump component modeled by a Poisson process, where jumps occur at a constant rate but at random and independently of each other. These jumps can be interpreted as the arrival of new information that significantly impacts the asset price rather than marginal fluctuations. Similar to the original Black-Scholes model, Merton's approach employs the risk-neutral probability measure, making the pricing independent of individual preferences

or expectations about future returns.

Building on Merton’s foundation, a broad literature has emphasized the importance of incorporating jumps into asset price modeling. A large body of these models continues to use Poisson-driven jumps, due to their relative simplicity and the fact that they allow for analytical solutions. For example, Bates (1996), Geman et al. (2001), and Zhou (2001) extend the jump–diffusion framework in various directions, showing how jump components can better explain empirical asset return distributions and option prices. A central model in which the jump component follows a Poisson process is Kou’s model (Kou, 2002). In this framework, jump sizes follow a double-exponential distribution, allowing for both upward and downward jumps in stock returns. This feature makes the model particularly well-suited to capturing the empirical tendency of stock returns to exhibit negative skewness. Unlike previous models, Kou’s model uses the real (physical) probability measure, which is essential for capturing the actual risk dynamics faced by investors. While the risk-neutral measure is primarily used for pricing, the real-world measure allows for the computation of meaningful risk metrics such as VaR, making it more suitable for risk management applications.

Using the risk-neutral measure, Carr and Wu (2003) propose a method to disentangle these components based on option pricing data. Their findings confirm that while both components exist, the jump component exhibits significant time variation. Furthermore, the role of jumps extends beyond asset returns to credit risk modeling. In contrast to the exogenous default framework considered in this paper, Chen and Kou (2009) introduce a model in which defaults occur endogenously. Their model is based on a GBM extended with two-sided jumps, where asset prices can experience both upward and downward discontinuous movements. This allows the model to capture the full range of market reactions, including sudden positive or negative shocks. In addition to modeling credit risk, their study explores the link between credit spreads, i.e., the yield premium demanded by investors to hold risky debt, and implied volatility, which refers to the market’s expectation of future volatility as inferred from option prices. While exogenous default models like this typically predict a positive relationship between credit spreads and implied volatility, they find that this link can break down when defaults are driven by a firm’s own value process and jump risks are present.

In contrast to Poisson-based models, Herbertsson (2025a) introduces a framework that does

not rely on a Poisson process for jump modeling. Instead, Herbertsson suggests a model with simultaneous jumps at defaults in an external group of defaultable entities. This hybrid risk model integrates both equity and credit risk, extending the analysis to risk management. By concentrating solely on negative jumps, it offers a more conservative estimate of VaR compared to models that account for both positive and negative jumps.

In Herbertsson (2025b), the author extends his work from 2023 by proposing a general model that allows for a portfolio where bonds issued by the exogenous defaultable entities are included. By also including the defaultable bond in the portfolio, the model is able to capture the double-negative effect resulting from the default (i.e., the actual loss from the default as well as the negative jump in equity price).

2.2 Credit Risk Modeling

A key concept in modeling credit risk is the default intensity, which quantifies the likelihood of default occurring at a given point in time. In the literature on jump-diffusion models, it is common to assume that the jump component is driven by a Poisson process. A Poisson process models the random arrival of discrete events over time, where the average frequency of events is known, but the exact timing is unpredictable. A defining feature of this process is its memorylessness, where the probability of an event occurring in the future is independent of the past.

This independence assumption does not align with the empirical fact that defaults tend to be correlated, especially during periods of market stress (Das et al., 2007). Given this assumption, it is unrealistic to model a sequence of, say, m defaults as the first m jumps of a Poisson process; see, for example, Section 3 in Herbertsson (2025b), particularly Theorem 3.3 and Corollary 3.4. To address this limitation, we instead model the default times of a group of m exogenous defaultable entities (such as corporates or sovereign states) directly, replacing the Poisson process with a more flexible default-time framework. This follows the approach in Herbertsson (2025b) and Herbertsson (2025a), but the framework is general enough to accommodate default times derived from any type of credit portfolio model.

To introduce dependence between these default times, various modeling techniques can be employed. A widely adopted approach is based on copula theory, which provides a flexible way

to model dependence between random variables. A copula links the marginal distributions of individual default times into a joint distribution, thereby capturing the structure of dependence across entities. As argued by Li (2000), when defaults exhibit dependence, it is essential to define a joint distribution over default times using a copula. This framework allows for modeling the dependence between defaults while keeping the individual marginal default behaviors unchanged.

A central question in the literature is which copula to choose. Malevergne and Sornette (2003) examine whether the Gaussian copula, one of the most commonly used models, adequately captures the dependence observed in financial returns. Based on empirical tests using data on currencies and stocks, they find that a key limitation of the Gaussian copula is its lack of tail dependence, which leads to an underestimation of the probability of simultaneous extreme losses, an important issue in risk management. Although the Gaussian copula appears acceptable for general dependence modeling, the authors caution that more flexible, non-Gaussian alternatives may be more appropriate in risk-sensitive contexts.

Further addressing these concerns, Kole et al. (2007) compare several copula families, including the Gaussian, Student's t , and Clayton copulas. Their empirical findings reinforce the view that the Gaussian copula is generally inadequate for capturing tail risk. In contrast, copulas such as the Clayton copula are shown to better account for asymmetric tail dependence, making them more suitable for modeling extreme events in financial markets.

2.3 Value-at-Risk

Among the most widely used approaches for quantifying financial risk is VaR, a statistical measure commonly applied in risk management to estimate the maximum potential loss over a given time horizon with a specified confidence level. Technically, VaR corresponds to a quantile of the loss distribution, that is, for a given confidence level α , the VaR is the smallest number x such that the probability of a loss not exceeding x is at least α . Duffie and Pan (1997) emphasize the importance of selecting a modeling framework that accurately captures the underlying dynamics of asset prices over the VaR horizon. In particular, they highlight the role of models that incorporate features such as jumps and time-varying volatility in improving the quality of VaR estimates. This is especially relevant when assessing portfolios subject to discontinuities

or sudden shocks.

While VaR has been subject to academic criticism, see Artzner et al. (1999), for not satisfying all the mathematical properties of a coherent risk measure, it remains a dominant tool in risk management. Alternative measures, such as Expected Shortfall (ES), have been proposed to address some of VaR's theoretical limitations by capturing the average loss beyond the VaR threshold. However, ES is often more challenging to estimate accurately, particularly in complex models with discontinuities or sparse tail data.

Grootveld and Hallerbach (1999) compare VaR and ES to traditional variance-based approaches and find that downside risk measures are more appropriate for non-normal return distributions. While ES can offer a more complete picture of tail risk, VaR continues to be a standard due to its computational tractability, regulatory acceptance, and strong interpretability in practical applications.

Although not explicitly applied in this thesis, VaR (and ES) is also widely used in portfolio optimization, where the objective is to minimize potential downside risk, see Gouriéroux et al. (2000) and Andersson et al. (2001). It is often considered a valuable alternative to variance-based models, as it captures the asymmetric and tail-risk nature of returns. While variance optimization penalizes both upward and downward deviations equally, VaR specifically targets losses, aligning more closely with the preferences of risk-averse investors.

In this thesis, we adopt VaR as the primary risk measure, motivated by its widespread use and the clear insights it provides into portfolio downside risk. Moreover, when carefully modeled, particularly under frameworks that account for jump risk and default dependence, VaR remains a robust and informative measure of financial risk.

3 Methodology

This section presents the methodology and underlying assumptions used in this study. Our analysis builds directly on the framework developed in Herbertsson (2025b), where portfolio risk measures are examined in a setting that includes both stocks and bonds, with stock prices subject to downward jumps at the default events of the bonds held in the portfolio. That study itself is an extension of the earlier work in Herbertsson (2025a), which focuses exclusively

on a stock portfolio affected by external credit events. For certain key calculations, e.g., the approximation of the number of defaults in the credit portfolio, we make use of methods and techniques introduced in Herbertsson (2023).

In Section 3.1, we outline the key assumptions and economic interpretations of Herbertsson’s model. Next, in Sections 3.1.1 and 3.1.2, we describe the modeling approaches for stock and bond prices, including how default risk is incorporated into asset dynamics. This is followed by a detailed treatment of the loss process in Section 3.1.3, which captures the impact of default events on portfolio value. In Section 3.1.4, we introduce the risk measure used in our analysis, VaR, and explain how it is computed within this framework. Finally, in Section 3.2, we present the saddlepoint approximation proposed by Herbertsson (2023), which is used to estimate the distribution of defaults. This is followed by a detailed explanation of the dependence structure between defaults using various copulas in Section 3.3.

3.1 Herbertsson’s Model

In this subsection, we present the model proposed by Herbertsson (2025b), which forms the foundation of this paper. The model is designed to capture joint equity-credit risk, which is the interdependence between stock and bond prices in the presence of credit events. Specifically, it is applied to a stock–bond portfolio in which the stock prices are subject to downward jumps at the moment when the corresponding bonds default. As previously mentioned, this paper builds on the framework developed in Herbertsson (2025a), where the analysis is limited to a pure stock portfolio. The model used for the mixed-asset configuration is a natural extension of that earlier framework, with the flexibility to set the bond share to zero, thereby reverting to the stock-only case.

Consistent with Herbertsson, our framework uses real-world (physical) probabilities rather than risk-neutral ones. This reflects the focus of our study on risk measurement rather than pricing. Modeling default events under physical probabilities allows us to base the analysis on historically observed likelihoods, providing a more realistic view of how risk evolves over time. This approach is well-suited for risk management applications, such as VaR estimation, where the goal is to assess potential future losses rather than determine fair market values. The model assumes a portfolio comprising two distinct sub-portfolios, one consisting of stocks and the other of bonds.

The stock sub-portfolio is treated as a large, homogeneous group, with all stocks sharing a common risk profile. This assumption of homogeneity simplifies the modeling of equity price dynamics across the portfolio and helps focus the analysis on the impact of defaults. The bond sub-portfolio, in contrast, consists of exchangeable defaultable bonds, meaning that each bond carries an identical probability of default. The exchangeability assumption eliminates distinctions between individual bonds, enabling a tractable modeling of the distribution of defaults within the bond sub-portfolio. In the model, the bonds are structured to pay a single lump sum amount at maturity, which exceeds the nominal value to reflect a positive yield. This approach effectively replicates the economic role of a coupon, acknowledging that zero-coupon bonds are typically issued at a discount to par. By incorporating this feature, the model captures a more realistic investment incentive, as bonds without any return component would be unattractive to investors. Moreover, the assumptions of a large, homogeneous portfolio of stocks and exchangeability among the bonds enhance the model’s traceability, enabling a more efficient analytical framework.

A key condition in this context is that the bonds are not issued by the same entities whose stocks populate the equity sub-portfolio. This ensures that default shocks remain exogenous, isolating the effects of bond defaults from endogenous interactions with the stock-issuing firms. Building on this foundation, we first apply the model by Herbertsson (2025b) to present the stock prices. Subsection 3.1.1, followed by the computation of bond prices, Subsection 3.1.2. These steps provide the basis for calculating the loss process and associated risk measure, e.g., VaR, achieved through numerical methods that leverage the default distribution. To capture the dependence between default times, we employ copula-based approaches, specifically the one-factor Gaussian copula, Subsection 3.3.1, and the Clayton, Subsection 3.3.2. These copulas differ in how they model dependence structure, offering valuable insights into varying risk scenarios.

3.1.1 Modelling Stock Prices

Within the framework proposed by Herbertsson (2025b), the stock price dynamics are modeled for a homogeneous stock sub-portfolio comprising J exchangeable entities A_1, \dots, A_J that do not belong to the bond sub-portfolio, which instead consists of a group of m defaultable entities C_1, \dots, C_m , with individual default times τ_1, \dots, τ_m . An essential feature of Herbertsson’s model is that the stock prices $S_{1,t}, \dots, S_{J,t}$ are affected by bond defaults through downward jumps, which

occur simultaneously across all stocks in the portfolio at the moment a bond defaults. Although stock prices could theoretically exhibit both positive and negative jumps, we follow Herbertsson (2025b) in focusing exclusively on negative jumps, as this study focuses on external credit risk. By only considering negative jumps, the model adopts a conservative stance, amplifying estimated risk measures such as VaR. The magnitude of these downward jumps is stochastic, following an exponential distribution, thereby ensuring that extreme losses, though rare, are captured within the model. For each entity A_j , if $S_{t,j}$ represents its stock price at time t , its evolution follows:

$$S_{t,j} = S_{0,j} \exp \left(\left(\mu_j - \frac{1}{2} \sigma_j^2 \right) t + \sigma_j \left(\rho_{S,j} W_{t,0} + \sqrt{1 - \rho_{S,j}^2} W_{t,j} \right) - \sum_{n=1}^{N_t^{(m)}} U_{n,j} \right) \quad (1)$$

where μ_j is the drift, σ_j is the volatility, and $\rho_{S,j} \in [-1, 1]$ determines the exposure of stock j to the common Brownian motion $W_{t,0}$. The processes $W_{t,0}, W_{t,1}, \dots, W_{t,J}$ are independent standard Brownian motions. The term $N_t^{(m)} = \sum_{i=1}^m \mathbf{1}_{\{\tau_i \leq t\}}$ counts the number of defaults among the m exogenous entities up to time t , with default times τ_1, \dots, τ_m . Each jump size $U_{n,j} \sim \text{Exp}(\eta_j)$ follows an exponential distribution with rate parameter $\eta_j > 0$, introducing downward jumps in stock prices upon default. Dependence among stocks arises both from the shared Brownian driver $W_{t,0}$ and the fact that all stocks are affected by the same set of default events $\{\tau_i\}$.

While the formulation in (1) is convenient for analytical purposes, especially when deriving closed-form expressions or proving properties of the process, it is less transparent in terms of how defaults affect individual stock prices. To clarify the role of defaults, we introduce an i.i.d. sequence $\tilde{U}_{1,j}, \dots, \tilde{U}_{m,j}$, distributed as $U_{1,j}$, and observe that the aggregate jump term can equivalently be written as $\sum_{i=1}^m \tilde{U}_{i,j} \mathbf{1}_{\{\tau_i \leq t\}}$. This expression makes explicit the association between each individual jump and its corresponding default event. Substituting this into the dynamics yields the alternative representation:

$$S_{t,j} = S_{0,j} \exp \left(\left(\mu_j - \frac{1}{2} \sigma_j^2 \right) t + \sigma_j \left(\rho_{S,j} W_{t,0} + \sqrt{1 - \rho_{S,j}^2} W_{t,j} \right) - \sum_{i=1}^m \tilde{U}_{i,j} \mathbf{1}_{\{\tau_i \leq t\}} \right). \quad (2)$$

Equation (2) is mathematically equivalent to (1), but it offers a more intuitive interpretation: each time a default τ_i occurs, the stock price experiences a relative drop of magnitude $1 - e^{-\tilde{U}_{i,j}}$.

Since $\tilde{U}_{i,j} \sim \text{Exp}(\eta_j)$, the jump sizes are strictly positive and typically lie within a range that corresponds to realistic loss sizes observed during market stress. The modeling approach is consistent with the framework of Herbertsson (2025a), and although it is possible to allow firm-specific jump size distributions by assigning different rate parameters η_j to each stock j , the generalization greatly complicates the derivation of analytical results, see Remark 4.3 of Herbertsson (2025a).

The framework is constructed under the real (physical) probability measure \mathbb{P} , as opposed to the risk-neutral measure \mathbb{Q} . This distinction is critical because the primary focus is on risk management rather than asset pricing. The expected stock price under the real measure incorporates both systematic and default-driven risks, see Herbertsson (2025b), given by:

$$\mathbb{E}[S_{t,j}] = S_0 e^{\mu_j t} \mathbb{E} \left[\left(\frac{\eta_j}{\eta_j + 1} \right)^{N_t^{(m)}} \right] = S_0 e^{\mu_j t} \sum_{k=0}^m \left(\frac{\eta_j}{\eta_j + 1} \right)^k \mathbb{P}[N_t^{(m)} = k] \quad (3)$$

where η_j is defined as the jump parameter that quantifies the reduction in stock price following a default, with a lower value of η_j indicating larger jumps and thus greater loss. The random variable $N_t^{(m)}$ counts the total defaults among the m defaultable entities C_1, \dots, C_m by time t . The summation over k from 0 to m applies the law of total expectation by conditioning on the total number of defaults that have occurred by time t . For each possible value of k , the term $\left(\frac{\eta_j}{\eta_j + 1} \right)^k$ represents the conditional effect on the stock price given that exactly k defaults have occurred. This is then weighted by the probability of observing k defaults under the real-world probability measure \mathbb{P} , expressed as $\mathbb{P}[N_t^{(m)} = k]$. The sum thus captures the expected value over all possible default scenarios, accounting for both the impact of each scenario and its likelihood.

Following the assumption of a homogeneous stock sub-portfolio, the stock prices $S_{t,1}, \dots, S_{t,J}$ of all firms A_1, \dots, A_J satisfy:

$$S_{0,j} = S_0, \quad \mu_j = \mu, \quad \sigma_j = \sigma, \quad \rho_{S,j} = \rho_S, \quad \eta_j = \eta$$

which means that all stocks in the sub-portfolio are assumed to be identical in terms of initial price, drift, volatility, correlation with the market, and sensitivity to default events. This

homogeneity assumption simplifies the analysis by allowing us to treat the stocks symmetrically. We estimate the jump parameter η to account for the impact of default events on the stock prices. This adjustment ensures that the expected stock price $\mathbb{E}[S_{T,j}]$ matches a specific target after a set time period, given by:

$$\mathbb{E}[S_{T,j}] = S_0 \quad \text{or equivalently} \quad \mathbb{E} \left[\left(\frac{\eta}{\eta + 1} \right)^{N_T^{(m)}} \right] = e^{-\mu T} \quad \text{for } T = 1. \quad (4)$$

This condition means that η is chosen so that the expected reduction from defaults balances the stock's growth rate μT over one year, keeping the expected stock price at S_0 . Equation (3) and (4) implies that the following must hold:

$$\sum_{k=0}^m \left(\frac{\eta_j}{\eta_j + 1} \right)^k \mathbb{P}[N_t^{(m)} = k] = e^{-\mu T}. \quad (5)$$

Equation (5) is used to solve for the corresponding value of η . Obviously, the value of η depends on how the default probabilities $\mathbb{P}[N_t^{(m)} = k]$ is being modeled, which is discussed further in Subsection 3.2 and 3.3.

3.1.2 Modelling Bond Prices

As pointed out in Herbertsson (2025b), pricing bonds under the real probability measure typically introduces additional complexity. The main challenge in real-world pricing is that, under this measure, investor risk preferences must be accounted for, requiring the use of a stochastic discount factor instead of simple discounting at the risk-free rate. To simplify computations, we follow the setup in Herbertsson (2025b) and assume that bond prices under the real-world measure coincide with those under the risk-neutral measure. While this assumption does not fully capture real-world pricing dynamics, it provides a useful approximation that makes the analysis more tractable.

In reality, zero-coupon bonds are typically purchased at a discount to their nominal value, offering a positive yield at maturity if the issuer avoids default. To capture this dynamic in a practical framework, we adopt the bond pricing model developed by Herbertsson (2025b), where a group of m entities C_1, \dots, C_m each issue a simple fixed-income bond with nominal value N_B ,

maturity T , and zero recovery upon default. This zero-recovery assumption is made to simplify the computations while still capturing the key features of credit risk in the valuation. The bond does not pay interim coupons, but accrues interest continuously over time through a coupon rate $c > 0$, which is expressed as a percentage of the nominal value. The price of the bond for the entity C_i at time $t \leq T$ is then defined under the real probability measure as:

$$B_{t,i} = 1_{\{\tau_i > t\}} N_B (1 + ct) \quad \text{for } t \leq T. \quad (6)$$

Here, τ_i denotes the default time of entity C_i , and $1_{\{\tau_i > t\}}$ is an indicator function equal to 1 if the entity has not defaulted by time t , that is, we assume no recovery at defaults. It is also clear that $B_{t,i} = 0$ if $\tau_i \leq t$, i.e., the price of the bond will be zero if C_i defaults before time t . The price function reflects the full value of the bond, including the accrued interest up to time t , that is, the bond is modeled using the dirty price, which incorporates both the principal (nominal value) and the accumulated coupon. Modeling the dirty price directly simplifies the analysis and aligns with our objective of capturing the full economic value of the bond over time, see Brown (2006), and Cairns (2004).

To characterize portfolio-level exposures, we define the aggregate number of surviving entities at time t as $N_t^{(m)} = \sum_{i=1}^m 1_{\{\tau_i \leq t\}}$. The total value of the bond portfolio at time t is then proportional to the number of non-defaulted entities, each priced according to (6).

At $t = 0$, the bond price is $B_{0,i} = N_B$, representing the initial investment. If entity C_i remains solvent until maturity, the price at time T becomes $B_{T,i} = N_B(1 + cT)$, generating a profit of $N_B cT$. The continuous coupon rate c implies that the bond accrues value steadily over time, but instead of interim payments, the total accrued coupon $N_B cT$ is paid at maturity alongside the principal, assuming no default has occurred.

3.1.3 Portfolio Loss Process

In this section, we describe the methodology for computing the value of the stock-bond portfolio and deriving its corresponding loss process. The portfolio value reflects the combined dynamics of stock prices and bond valuations introduced in earlier sections, while the loss process quantifies the effects of bond defaults and the associated jumps in stock prices. The loss process will be

used in the computation of risk measures, such as VaR, by shaping the distribution of potential portfolio losses.

For a portfolio consisting of bonds from m different defaultable entities and stocks from J different exchangeable companies, and where the stock and bond prices follows what was outlined in Subsection 3.1.1 and 3.1.2, the portfolio value V_t and loss process L_t , at time t can be defined as:

$$V_t = \sum_{j=1}^J w_j S_{t,j} + \sum_{i=1}^m \omega_i B_{i,t} \quad \text{and} \quad L_t = -(V_t - V_0)$$

where w_j is the number of shares owned of each company j and ω_i is the number of each bonds owned from each defaultable entity i . For an equally weighted portfolio, or with the homogeneity assumption as used by Herbertsson (2025b), the weights simplifies to $w = w_1 = \dots = w_J$ and $\omega = \omega_1 = \dots = \omega_m$. Using the expression for bond prices from Equation (6), the portfolio value V_t at time t can be rewritten as:

$$V_t = w \sum_{j=1}^J S_{t,j} + \omega \sum_{i=1}^m 1_{\{\tau_i > t\}} N_B (1 + ct). \quad (7)$$

At the initial time $t = 0$, when no defaults have occurred (i.e., $N_0^{(m)} = 0$), the portfolio value simplifies to $V_t = wJS_0 + \omega mN_B$, where S_0 is the initial stock price, assumed uniform across all stocks. This expression remains valid even when a coupon is present, as in (6), since the coupon term vanishes at $t = 0$. This is consistent with the intuition that no interest has accrued at the initial time. We follow the setup in Herbertsson (2025b) and define the initial portfolio allocation such that stocks constitute $100\gamma\%$ of the total value, and bonds account for $100(1 - \gamma)\%$, where $\gamma \in [0, 1]$ is a constant. These proportions are expressed as fractions of the initial portfolio value, given by:

$$\gamma = \frac{wJS_0}{V_0} \quad \text{and} \quad 1 - \gamma = \frac{\omega mN_B}{V_0}. \quad (8)$$

In the portfolio model, the parameters w and ω serve as scaling constants for the equity and bond components. As noted by Herbertsson (2025b), it is possible to set $w = \omega = 1$ without

changing the behavior of the model. This simplification allows us to rewrite Equation (8) as follows:

$$N_B = \frac{JS_0(1-\gamma)}{m\gamma} \quad \text{and} \quad V_0 = \frac{JS_0}{\gamma}. \quad (9)$$

Using the simplified equations (7), (8), and (9), it is now possible to express the value of the portfolio at time t and the loss process in terms of the components of the portfolio's equity and bonds, defined as (for details, see Herbertsson (2025a)):

$$V_t = \sum_{j=1}^J S_{t,j} + \frac{JS_0(1-\gamma)}{m\gamma}(1+ct) \left(m - N_t^{(m)} \right)$$

and

$$L_t = JS_0 - \sum_{j=1}^J S_{t,j} + \frac{JS_0(1-\gamma)}{m\gamma} \left((1+ct)N_t^{(m)} - mct \right).$$

The portfolio value V_t reflects the current worth of the stocks $\sum_{j=1}^J S_{t,j}$ and the remaining bonds. The bond component of the portfolio is affected by the number of defaults. If $N_t^{(m)}$ bonds have defaulted by time t , then the number of remaining bonds is $m - N_t^{(m)}$, and each of these bonds has the nominal value N_B .

The loss process, where $L_t = -(V_t - V_0)$, captures the decline in value due to falling stock prices and bond defaults. Specifically, the stock contribution to the loss, $JS_0 - \sum_{j=1}^J S_{t,j}$, represents the difference between the initial stock value and the value at time t , which can be positive or negative. The bond contribution, $N_t^{(m)} \frac{JS_0(1-\gamma)}{m\gamma} \left((1+ct)N_t^{(m)} - mct \right)$, reflects the losses from bond defaults and since $N_t^{(m)} \geq 0$, as long as $0 < c$, this can be either positive or negative. However if $c = 0$, it can only be positive, indicating that the bonds can only decrease the loss if they do not have a coupon value.

3.1.4 Value-at-Risk

VaR is one of the most widely used risk measures in financial risk management. It estimates the potential loss in a portfolio over a given time horizon at a specified confidence level α . VaR provides a single summary statistic that quantifies the downside risk of a portfolio. Specifically for a confidence interval α , the VaR represents the smallest loss level such that the probability

of incurring a larger loss is no more than $1 - \alpha$. Formally, for a random loss variable L_t , the VaR at level α is defined as:

$$\text{VaR}_\alpha(L_t) = \inf\{y \in \mathbb{R} : \mathbb{P}[L_t > y] \leq 1 - \alpha\} = \inf\{y \in \mathbb{R} : F_{L_t}(y) \geq \alpha\}$$

where $F_{L_t}(x) = \mathbb{P}[L_t \leq x]$ represents the cumulative distribution function of the loss at time t , and α is the significance level. Finding analytical expressions for $F_{L_t}(x)$ can often be challenging, however, Herbertsson (2025b) provides the following approximation of $F_{L_t}(x)$ assuming the number of stocks J is large:

$$\mathbb{P}[L_t \leq x] \approx 1 - \sum_{k=0}^m \Psi_k^{(\gamma)}(x, t, J, m, c, \eta, s) \mathbb{P}[N_t^{(m)} = k] \quad (10)$$

where $\mathbf{s} = (\mu, \sigma, S_0, \rho_S)$, and $\Psi_k^{(\gamma)}(x, t, J, m, \eta, \mathbf{s})$ is defined for each k as

$$\Psi_k^{(\gamma)}(x, t, J, m, c, \eta, s) = \Phi\left(\frac{\ln G(x, t, k, \gamma, c) - \left(\mu - \frac{1}{2}\sigma^2 p_s^2\right)t}{\sigma p_s \sqrt{t}}\right)$$

with $G(x, t, k, \gamma, c)$ given by:

$$G(x, t, k, \gamma, c) = \left(D(\gamma, t, k, c) - \min\left(\frac{x}{J_0}, D(\gamma, t, k, c)\right)\right) \left(\frac{\eta + 1}{n}\right)^k$$

and $D(\gamma, t, k, c)$ defined as:

$$D(\gamma, t, k, c) = 1 + \frac{1 - \gamma}{m\gamma} ((1 - ct)k - mct)$$

where $\Phi(x)$ is the standard normal cumulative distribution function and $N_t^{(m)}$ denotes the number of exogenous defaults up to time t under the model assumptions. The probability $\mathbb{P}[N_t^{(m)} = k]$ captures the likelihood of observing k defaults up to time t , and is further discussed in Section 3.2.

A special case of this model is the model from Herbertsson (2025a) for large homogeneous stock portfolios, where the portfolio consists only of stocks, and therefore the default can be seen as

an exogenous event. This can be achieved by letting $\gamma = 1$, and Equation (10) simplifies as follows:

$$\mathbb{P}[L_t \leq x] \approx 1 - \sum_{k=0}^m \Phi \left(\frac{\ln \left(1 - \frac{x}{JS_0} \left(\frac{\eta+1}{\eta} \right)^k \right) - \left(\mu - \frac{1}{2} \sigma^2 \rho_S^2 \right) t}{\sigma \rho_S \sqrt{t}} \right) \mathbb{P}[N_t^{(m)} = k].$$

Since the loss function L_t determines portfolio losses, VaR can be calculated using its cumulative distribution function (CDF). Using the large portfolio approximation $\mathbb{P}[L_t \leq x] \approx F_{L_t}^{LPA}(x)$, and if $\rho_S \neq 0$ Herbertsson (2025b) propose the solution x^* to $F_{L_t}^{LPA}(x^*) = \alpha$ as an approximation of $\text{VaR}_\alpha(L_t)$. This can also be formulated as:

$$\text{VaR}_\alpha(L_t) = \left(F_{L_t}^{LPA} \right)^{-1}(\alpha) \quad \text{for large } J$$

where $\left(F_{L_t}^{LPA} \right)^{-1}(\alpha)$ is the inverse function of the loss distribution. To solve the equation, we use the built-in MATLAB function `fzero`.

3.2 Saddlepoint Approximation for the Distribution of Defaults

In order to approximate the distribution of the number of defaults $\mathbb{P}[N_t^{(m)} = k]$ in the credit portfolio setting, we employ the saddlepoint approximation technique presented by Herbertsson (2023). This method is well-suited for estimating tail probabilities and probability mass functions of discrete distributions. The foundation of the approach lies in representing the number of defaults $N_t^{(m)}$ in a homogeneous credit portfolio as a sum of conditionally independent Bernoulli variables. The saddlepoint method yields accurate closed-form approximations for both the tail probability $\mathbb{P}[N_t^{(m)} \geq k]$, which measures the likelihood of observing at least k defaults by time t , and the point probability $\mathbb{P}[N_t^{(m)} = k]$ which gives the exact probability of observing exactly k defaults, where $k = 0, 1, 2, \dots, m$.

To estimate $p(t, z)$, we use the one-factor Gaussian copula model (see Subsection 3.3.1) and the Clayton Copula model (see Subsection 3.3.2). These models capture the fact that defaults are not independent by introducing a common underlying factor, denoted Z , which represents systematic risk affecting all firms. Given a specific value of this factor $Z = z$, the default

probability of a single firm becomes $p(t, z)$. Since the defaults are conditionally independent when Z is fixed, the number of defaults in the portfolio follows a binomial distribution with parameters m and $p(t, z)$.

The saddlepoint approximation for $\mathbb{P}[N_t^{(m)} \geq k]$ is defined using the following equations (for full derivations, see Herbertsson (2023)):

$$\mathbb{P}\left[N_t^{(m)} = k\right] = \mathbb{E}\left[\Delta H_B^{(\text{LR})}(k, m, p(t, Z))\right] + \mathcal{O}(m^{-3/2}) \quad (11)$$

where \mathcal{O} is an error term, and $\Delta H_B^{(\text{LR})}(k, m, p(t, Z))$ is defined as:

$$\Delta H_B^{(\text{LR})}(k, m, p(Z_t)) = \begin{cases} H_B^{(\text{LR})}\left(\frac{k}{m}, m, p(Z_t)\right) - H_B^{(\text{LR})}\left(\frac{k+1}{m}, m, p(Z_t)\right), & \text{for } k \leq m-1 \\ p(Z_t)^m, & \text{for } k = m \end{cases}$$

with $H_B^{(\text{LR})}(x, m, p)$ defined for $0 < x < 1$ and $p \neq x$ as:

$$H_B^{(\text{LR})}(x, m, p) = 1 - \Phi(\hat{w}_B) + \varphi(\hat{w}_B) \left(\frac{1}{\hat{z}_B} - \frac{1}{\hat{w}_B} \right)$$

where $x = \frac{k}{m}$, $p = p(Z_t)$ and where

$$\hat{w}_B = \hat{w}_B(x, m, p) = \text{sgn}(\hat{w}_B) \sqrt{2m \left(x \ln \left(\frac{x(1-p)}{(1-x)p} \right) - \ln \left(\frac{1-p}{1-x} \right) \right)}$$

with

$$\text{sgn}(\hat{w}_B) = \text{sgn} \left(\frac{x(1-p)}{(1-x)p} - 1 \right)$$

where

$$\hat{z}_B = \hat{z}_B(x, m, p) = \sqrt{mx(1-x)} \left(1 - \frac{(1-x)p}{x(1-p)} \right)$$

Furthermore, for $x = 0$ and $x = 1$, $H_B^{(\text{LR})}(0, m, p) = 1$ and $H_B^{(\text{LR})}(1, m, p) = p^m$. The expected value in Equation (11) is solved using the following integral:

$$\mathbb{P} \left[N_t^{(m)} = k \right] = \int_{-\infty}^{\infty} \Delta H_B^{(\text{LR})} (k, m, p(t, z)) f_{Z_t}(z) dz + \mathcal{O}(m^{-3/2}).$$

3.3 Copulas

In this subsection, we explore how copulas capture dependence between default times in portfolio risk models. We overview the role of copulas in connecting marginals to joint behavior, then compare the one-factor Gaussian copula, ideal for symmetric dependence, and the Clayton copula, focused on lower tail dependence for extreme events.

One effective approach to capture dependence in portfolio risk models is through copulas. These functions allow us to model how random variables, e.g., default times, depend on each other, separate from their individual marginal distributions. A wide range of copula functions exists (see Patton (2012)), each with unique statistical properties suited to different dependence patterns. These properties significantly influence the likelihood of joint defaults and the shape of the tail in the aggregate default loss distribution.

Given marginal default probabilities, the joint dependence structure can be specified using a copula, where the choice of copula determines the dependence. For instance, copulas exhibiting lower tail dependence, such as Clayton copulas, are more likely to generate simultaneous low values across multiple marginals, increasing the probability of clustered defaults and amplifying aggregate losses. Conversely, copulas with asymptotic independence, like the Gaussian copula, often fail to capture the risk of extreme joint defaults, as they distribute dependence more evenly and lack pronounced tail effects. Copulas are useful in applied settings due to their ability to construct a joint distribution by combining any set of marginal distributions with a chosen dependence structure. This allows us to break down a multivariate distribution into two components, the marginal distribution and the joint distribution.

3.3.1 One-factor Gaussian Copula

The Gaussian copula is one of the most widely used copulas in credit risk modeling, particularly in the context of portfolio credit risk and modeling default correlation. Its popularity stems from

its analytical tractability and its ability to represent symmetric dependence structures using a single correlation parameter. Since it uses the correlation coefficient ρ in the multivariate normal distribution to define the dependence, it can only model linear relationships.

Assuming that the default times of all m defaultable entities are exchangeable and conditionally independent, the conditional default probability up to time t for each entity C_i under the one-factor Gaussian copula model is given by:

$$\mathbb{P}[\tau_i \leq t|Z] = \Phi\left(\frac{\Phi^{-1}(F(t)) - \sqrt{\rho}Z}{\sqrt{1-\rho}}\right)$$

where Z is a standard normally distributed variable with mean zero and unit variance that represents a shared source of randomness affecting all entities C_i . It captures systematic risk and introduces dependence between the otherwise conditionally independent default events. Furthermore, ρ is the default correlation parameter, $\Phi(x)$ is the distribution function of a standard normal random variable, and the marginal default distribution $F(t)$ is given by $F(t) = \mathbb{P}[\tau_i \leq t] = 1 - e^{-\lambda t}$.

Recalling Equation (5) which is used to solve for η , and that $\mathbb{P}[N_t^{(m)} = k]$ is a function of the individual default probability of all firms, we see that the value of η under the one-factor Gaussian Copula depends on the value of ρ . Therefore, keeping all else equal, one can study the relationship between ρ and η , which is done by Herbertsson (2025b).

3.3.2 Clayton Copula

In this subsection, we follow the same notation and modeling framework as in Herbertsson (2025a), where the Clayton copula is applied to capture default dependence across entities. The Clayton copula is particularly suited for modeling lower tail dependence, meaning it captures the tendency for extreme losses in one variable to occur alongside extreme losses in another. This property is especially relevant in credit risk, where defaults tend to cluster during periods of financial stress. Compared to the Gaussian copula, which lacks tail dependence, the Clayton copula provides a more realistic description of joint extreme events. However, it does not model upper tail dependence and is inherently asymmetric, focusing only on dependence in the lower tail. For a more detailed discussion of the Clayton copula and its properties in credit risk

modeling, see Burtschell et al. (2009) and Hofert and Scherer (2011).

Under the Clayton copula, the conditional default probability for each entity C_i with default time τ_i , given a random factor Z , is:

$$\mathbb{P}[\tau_i \leq t | Z] = \exp(Z(1 - F(t)^{-\theta}))$$

where $\theta > 0$ is defined as the Clayton copula parameter, controlling how strongly the default times are correlated, where higher θ implies greater dependence, meaning defaults are more likely to cluster together. Z is defined as a gamma-distributed random variable with density:

$$f_Z(z) = \frac{z^{\frac{1-\theta}{\theta}} e^{-z}}{\Gamma\left(\frac{1}{\theta}\right)} \quad \text{for } z \geq 0$$

with parameters $a = \frac{1}{\theta}$ and $b = \frac{1}{1-\theta}$. The factor (Z) defines dependence, where a large (Z) increases the conditional default probability for all entities, raising the likelihood of simultaneous defaults.

A key advantage of the Clayton copula is its explicit formula for default correlation between entities $i \neq j$:

$$\text{Corr} [1_{\{\tau_i \leq t\}}, 1_{\{\tau_j \leq t\}}] = \frac{\left(\frac{2}{F(t)^\theta} - 1\right)^{-\frac{1}{\theta}} - F(t)^2}{F(t)(1 - F(t))}$$

This correlation, derived from the Clayton copula's structure, measures the likelihood of joint defaults up to time t . In order to do a fair comparison of these results to those of the one-factor Gaussian copula, we align the two models by setting the marginal default probability $F(t) = \mathbb{P}[\tau_i \leq t]$ to match that of the Gaussian copula model, ensuring differences in VaR results arise from the dependence structure, and not individual default probabilities. Further, the Clayton copula parameter θ is calibrated so that the one-year default correlation, $\text{Corr}(1_{\{\tau_i \leq t\}}, 1_{\{\tau_j \leq t\}})$, equals that of the Gaussian copula for the corresponding correlation parameters ρ .

Unlike the Clayton copula, the Gaussian copula lacks an analytical default correlation formula. For calibration, we follow the method of Herbertsson (2025a), numerically computing the one-

year default correlation under the Gaussian copula. The analytical correlation formula of the Clayton copula is then inverted numerically to determine the corresponding value of θ . This ensures both models exhibit the same level of dependence at $t = 1$, allowing a direct comparison of VaR outcomes.

4 Results

In this section, we present the results obtained from applying the methods outlined in previous sections. First, in Section 4.1, we examine the distribution of defaults derived from the one-factor Gaussian copula and the Clayton copula, providing a comparative perspective on how the dependence structure via different copulas influences credit risk modeling. In Section 4.2, we present the key risk measure, VaR, under these two dependence structures: one-factor Gaussian copula (Section 4.2.1) and Clayton copula (Section 4.2.2). We analyze how VaR varies across different portfolio configurations and parameters, such as asset allocation and correlation.

4.1 Default Distribution

4.1.1 Default Distribution under the One-Factor Gaussian Copula

To visualize how the probability distribution of the number of defaults $\mathbb{P}[N_t^{(m)} = k]$ evolves over time t under the one-factor Gaussian copula framework, we present Figure 1. Using MATLAB’s built-in `binopdf` function, we compute the probability of observing k defaults at each time point t , under the assumption of a one-factor Gaussian copula model. The parameters used in the computations rendering Figure 1 are given in Table 1.

ρ_1	ρ_2	$F(t)$	λ	$\mathbb{P}[\tau_i \leq 1]$	S_0	μ	σ	ρ_s	m	J
0.3	0.6	$1 - e^{-\lambda t}$	0.0335	0.0329	50	0.15	0.2	0.25	125	150

Table 1: Parameters and related quantities for the one-factor Gaussian copula model.

We test two different values for the default correlation parameter in the one-factor Gaussian correlation model, denoted by ρ_1 and ρ_2 , to assess the impact of varying levels of dependence between the defaultable bonds in the portfolio. A higher value of ρ implies stronger correlation, meaning that if one bond defaults, the likelihood of additional defaults increases. The function $F(t)$ represents the marginal default probability distribution for each obligor, that is $F(t) =$

$\mathbb{P}[\tau_i \leq t]$, where the default times τ_1, \dots, τ_m have the same distribution for all C_1, \dots, C_m due to the exchangeability assumption. Just as in Herbertsson (2025a), $F(t)$ is specified as an exponential distribution, $F(t) = 1 - e^{-\lambda t}$, where λ is the constant default intensity, i.e. each τ_i has a constant default intensity λ . Consequently, $\mathbb{P}[\tau_i \leq 1]$ corresponds to the unconditional one-year default probability for a representative obligor. The parameters S_0 , μ , and σ describe the initial level, drift, and volatility of the underlying credit spread process.

It is important to note that this thesis does not aim to estimate the specific parameter values used in the modeling framework. Instead, the primary objective is to derive analytical expressions for key risk measures related to stock-bond portfolios, which will subsequently serve as the foundation for analyzing the time evolution of VaR. While certain parameters will be varied to assess their influence on VaR, the study does not involve a formal calibration procedure. For a detailed justification of the parameter choices, we refer to the work of Herbertsson (2025a), where each value is motivated and shown to be consistent with empirically observed financial conditions.

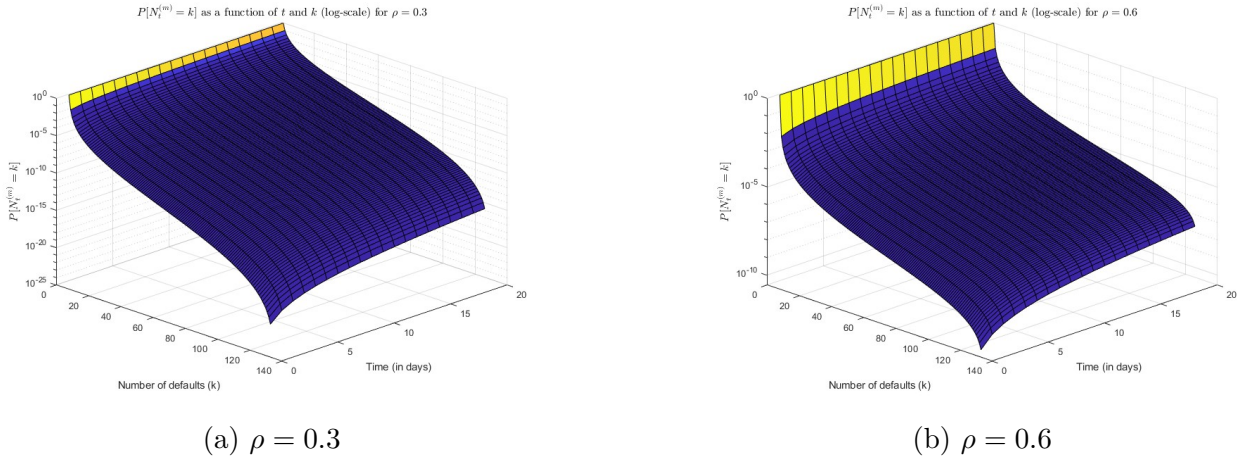


Figure 1: Probability distribution of the number of defaults $\mathbb{P}[N_t^{(m)} = k]$ over time t , where $t = 1, 2, \dots, 20$ days, using the one-factor Gaussian copula model, shown on a log scale for two correlation levels, $\rho_1 = 0.3$ (left) and $\rho_2 = 0.6$ (right).

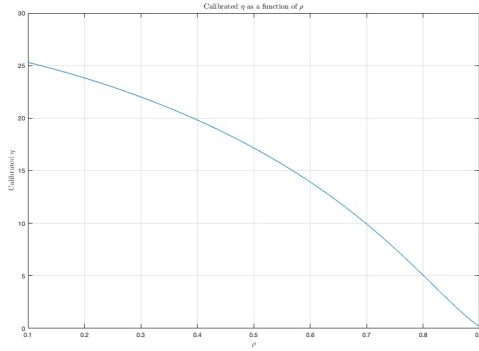
Figure 1a shows the probability of observing exactly k defaults at each time point t (in this case, each day), denoted $\mathbb{P}[N_t^{(m)} = k]$. The plot uses a logarithmic scale and presents this probability as a function of time t (in days, ranging from 1 to 20) and the number of defaults k (ranging from 0 to 125). The correlation parameter ρ_1 is set to 0.3. For each fixed t , the probabilities of all possible default outcomes k sum to one. Note that in Figures 1 and 3, the time t is shown

in days, but the calculations of the default probabilities $\mathbb{P}[N_t^{(m)} = k]$ are based on t measured in years, consistent with Herbertsson (2025a). For instance, 1, 5, and 20 days correspond to $t = \frac{1}{252}$, $t = \frac{5}{252}$, and $t = \frac{20}{252}$, using 252 as the average number of trading days. Much of the analysis in this paper focuses on 5 and 20 days VaR, which is supposed to represent weekly and monthly VaR in trading days.

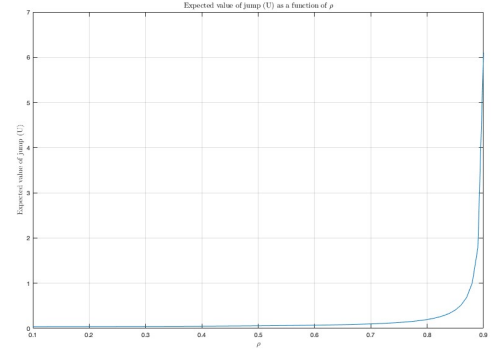
A clear pattern that emerges is that the probability of observing a large number of defaults is significantly lower at earlier time points. This is evident when we fix an early value of t and examine how the probability $\mathbb{P}[N_t^{(m)} = k]$ decays as the number of defaults k increases. This is expected, as a high number of defaults occurring within just a few days would imply that nearly all firms in the portfolio defaulted in a short time frame, which is an extremely rare event.

As time progresses, the probability of a higher number of defaults increases, reflecting the natural accumulation of risk over a longer horizon, i.e. $F(t) = \mathbb{P}[\tau_i \leq t]$ is increasing with time t . Conversely, for a fixed time t , the probability increases as we move from higher values of k (i.e., more defaults) toward lower values, which is consistent with the intuitive expectation that fewer defaults are more likely than many.

Figure 1b shows the default distribution $\mathbb{P}[N_t^{(m)} = k]$ with a higher correlation parameter, $\rho_2 = 0.6$. Increasing ρ amplifies the dependence between obligors, which in turn increases the likelihood of default clustering, i.e., the occurrence of multiple defaults within a short time span. This effect is visible in the right plot, where the probability mass shifts toward higher values of k for all t , indicating a greater risk of simultaneous defaults compared to the lower-correlation case shown in the left plot. Note that Figure 1a is similar to the corresponding graph in Figure 4 in Herbertsson (2025a) and this leads to confidence in our numerical implementation of the computations of $\mathbb{P} \left[N_t^{(m)} = k \right]$.



(a) Calibrated η using Equation (5) for $T = 1$ as function of one-factor Gaussian correlation parameter ρ .



(b) Expected value of jumps $E[U_n] = \frac{1}{\eta}$ in log of stock prices as a function of one-factor Gaussian correlation parameter ρ .

Figure 2: Calibrated η and expected value of jumps $E[U_n]$ as function of ρ .

Figure 2a shows how the calibrated value of the jump parameter η varies with the one-factor Gaussian copula correlation parameter ρ , where the calibration of η is done using Equation (4), or equivalently using Equation (5). The parameter η governs the magnitude and likelihood of downward jumps in the stock price after a default. A higher η implies smaller jumps (less severe spillover), while a lower η corresponds to more significant expected jumps. As we can see in Figure 2a, η decreases as ρ increases. This reflects the fact that, under higher dependence (larger ρ), a stronger contagion effect is needed to match the same expected loss level, meaning more pronounced jumps (lower η) are required.

In Figure 2b, we show how this relationship influences the expected log-price jump $\mathbb{E}[U_n]$. As ρ increases (and η decreases), the expected downward jump becomes more severe. Notably, when ρ exceeds a certain threshold, η approaches zero, causing $\mathbb{E}[U_n]$ to increase sharply. For high values of η and fixed μ , Equation (5) may have no real solution. To avoid this non-existence issue, we restrict our calibration and numerical analysis to $\rho \leq 0.9$, ensuring that a valid value of η always exists for the baseline case of $\mu = 0.15$, and similar observations are made in Herbertsson (2025a) and Herbertsson (2025b).

4.1.2 Default Distribution under the Clayton copula

Next, we analyze the probability distribution of the number of defaults using the Clayton copula. The parameters we use are summarized in Table 2. As previously noted, a detailed motivation for the selection of these specific parameter values is provided in Herbertsson (2025a). Recall-

ing 3.3.2, the Clayton copula parameter θ is calibrated so that the pairwise default correlation matches the corresponding pairwise default correlation for the one-factor Gaussian copula correlation parameter ρ , allowing for a direct comparison with the one-factor Gaussian copula.

θ_1	θ_2	$F(t)$	λ	$\mathbb{P}[\tau_i \leq 1]$	S_0	μ	σ	ρ_s	m	J
0.169	0.44	$1 - e^{-\lambda t}$	0.0335	0.0329	50	0.15	0.2	0.25	125	150

Table 2: All model parameters and values for the Clayton copula and stock price dynamics $S_{t,j}$.

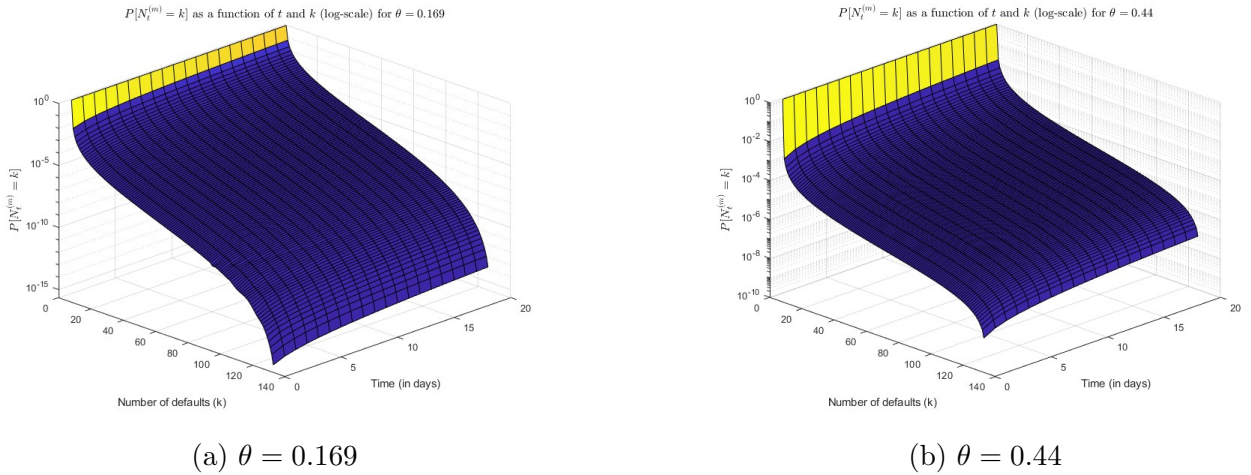
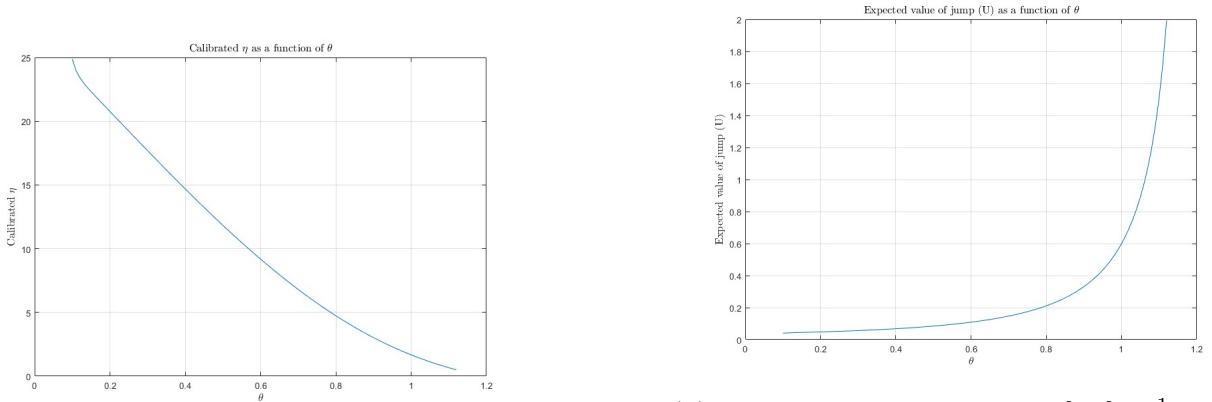


Figure 3: Default probability distribution $\mathbb{P}[N_t^{(m)} = k]$ as a function of time t , where $t = 1, 2, \dots, 20$ days, and the number of defaults k , shown on a log scale. The plots are based on the Clayton copula model for two different dependence parameters: $\theta_1 = 0.169$ (left) and $\theta_2 = 0.44$ (right).

We observe similar behavior in the default probabilities under the Clayton copula, where the surface declines sharply as the number of defaults k increases. This suggests that the probability of observing a large number of defaults remains low. To compare the Clayton copula with the one-factor Gaussian copula model, we examine two specific cases: Figure 3a, which corresponds to $\theta_1 = 0.169$, is compared with the Gaussian model in Figure 1a, where $\rho = 0.3$. Similarly, Figure 3b, with $\theta_2 = 0.44$, is compared with Figure 1b, corresponding to $\rho = 0.6$. Similar values for θ are also obtained in Herbertsson (2025a). Recalling the discussion in Section 3.3.2, the θ values have been calibrated to match the same pairwise default correlation as the corresponding ρ values, enabling a meaningful comparison between the two dependence structures.

In both comparisons, the Clayton copula exhibits a higher probability of clustered defaults, especially in the early stages of the time horizon. This is due to its lower tail dependence,

which increases the likelihood of joint extreme events. In contrast, the one-factor Gaussian copula does account for correlation between entities, but it does not capture this kind of tail dependence. Although increasing ρ in the Gaussian model strengthens the overall dependence, it still fails to replicate the same level of joint default risk observed in the Clayton model. This makes the Clayton copula more suitable for capturing systemic events, where many defaults occur simultaneously due to shared exposure to extreme shocks.



(a) Calibrated η using Equation (5) for $T = 1$ as function of Clayton parameter θ .

(b) Expected value of jumps $E[U_n] = \frac{1}{\eta}$ in log of stock prices as function of Clayton parameter θ .

Figure 4: Calibrated η and expected value of jumps $E[U_m]$ as function of θ .

Similarly to Figure 2, we see in Figure 4 that as we increase the dependence parameter θ used under the Clayton framework (ρ in the one-factor Gaussian copula case) η decreases, which causes the expected downward jump in the stock prices $E[U_n]$ to increase. This means that as the tail risk increases, a larger downward jump in stock prices is required for Equation (4) to hold. Using the same arguments as in the previous section, we limit our analysis to studying only when $\theta \leq 1.12$ to ensure that there always exists a solution to Equation (5) when $\mu = 0.15$.

4.2 Value at Risk

In the following section, we present results related to the VaR for various portfolio compositions under different default dependence structures. While a 20-day horizon is commonly used in equity risk assessment and is applied here to examine the time evolution of VaR, we also compute VaR at fixed time points, specifically at 5 and 20 days, to isolate and assess the effects of portfolio structure and asset dependence. This approach enables us to draw conclusions about

how these factors influence the estimated risk, independently of the time horizon. In Section 4.2.1, we present numerical results based on default times modeled using a one-factor Gaussian copula, while Section 4.2.2 contains corresponding results under the Clayton copula.

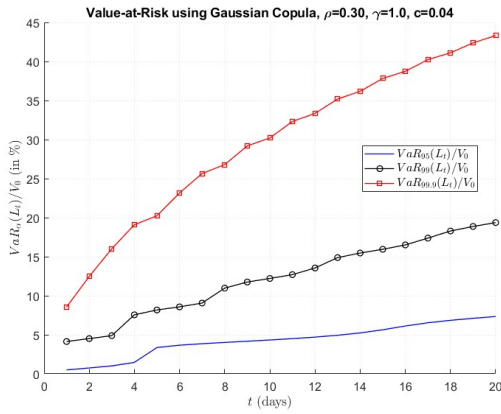
4.2.1 Value at Risk Estimation Using the One-Factor Gaussian Copula

In this section, we present numerical examples of VaR when the default times are driven by a one-factor Gaussian copula model. The portfolio configurations are presented in Table 3 (for a detailed motivation behind the parameter values, see Herbertsson 2025b). These parameters are used in all the following examples unless otherwise stated. The coupon rate is set to $c = 0.04$ and can be interpreted as a continuously accruing coupon, expressed as a proportion of the nominal value, with the total accrued amount paid as a lump sum at maturity T . We will later vary the coupon rate at fixed time points to evaluate its impact on the VaR.

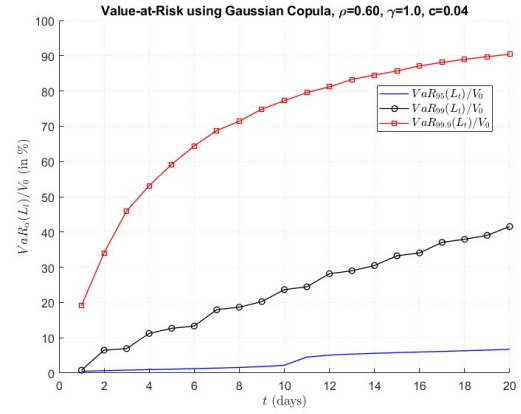
J	m	μ	σ	S_0	ρ_s	λ	c
150	125	0.15	0.2	50	0.25	0.0335	0.04

Table 3: Model parameters and their values for the one-factor Gaussian copula model and the Clayton copula model.

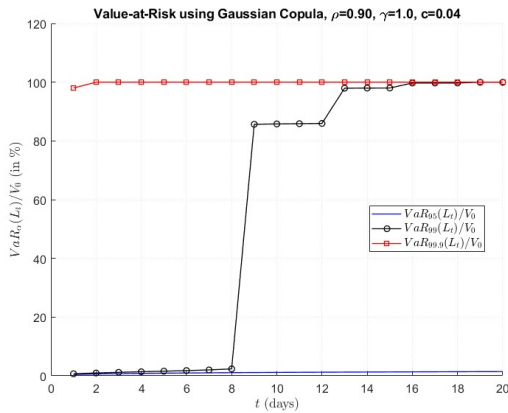
First, we evaluate the evolution of VaR for a portfolio containing only stocks, that is $\gamma = 1$, modeled using a one-factor Gaussian copula, examining the impact of varying the correlation parameter, ρ . The VaR is computed at confidence levels of 95%, 99%, and 99.9%, and we analyze how changes in ρ influence the resulting risk measure. Additionally, we include a plot illustrating the relative difference in VaR from Figure 5a and the VaR derived from the Black and Scholes, 1973 model, at the same confidence levels. VaR is computed for $t = 1, 2, \dots, 20$ days. The y-axis in Figures 5a to 5c shows the VaR for the given confidence level, divided by the initial value of the portfolio, resulting in a percentage loss relative to the starting value.



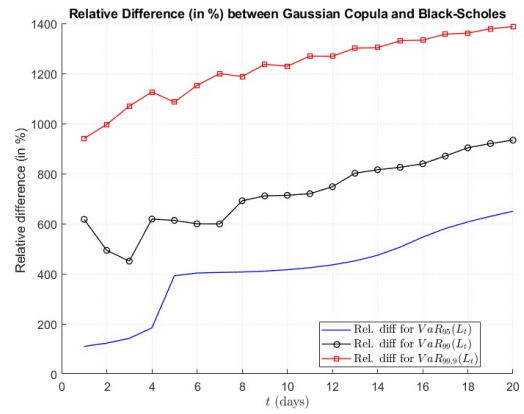
(a) $\rho = 0.3$



(b) $\rho = 0.6$



(c) $\rho = 0.9$



(d) Relative difference between VaR from Herbertsson (2025b) model for $\rho = 0.3$ and Black and Scholes (1973) model (in % of Black-Scholes VaR).

Figure 5: Comparison of Value-at-Risk (in % of V_0) for different values of ρ and relative difference between VaR from Herbertsson (2025b) model and Black and Scholes (1973) model (in %), with parameters given in Table 3.

The discontinuous behavior observed in the VaR curves in Figures 5a to 5c is mainly due to the stepwise nature of the default counting process $N_t^{(m)}$, which models the number of defaults over time. Since the analysis is conducted over a short horizon, the probability of no defaults is high, resulting in somewhat flat segments in the VaR curve. When a default does occur, the loss jumps abruptly, causing a visible discontinuity. This pattern arises because, over short time intervals, the distribution of $N_t^{(m)}$ is highly concentrated at zero, meaning that defaults are rare but have a large impact when they occur. As the time horizon increases, the likelihood of multiple defaults grows, and the distribution becomes more dispersed. This leads to a smoother evolution of the

VaR curves. Similar observations of the discontinuous behavior of the VaR-curves are made in Herbertsson (2025a).

It is clear from the plots in Figure 5 that increasing the correlation parameter, ρ , significantly changes the time evolution pattern of VaR. In Figure 5a, where we set a relatively conservative correlation of $\rho = 0.3$, we observe a stable increase in VaR over time. The most pronounced growth occurs at the 99.9% confidence level, as expected, since this level captures the most extreme tail events.

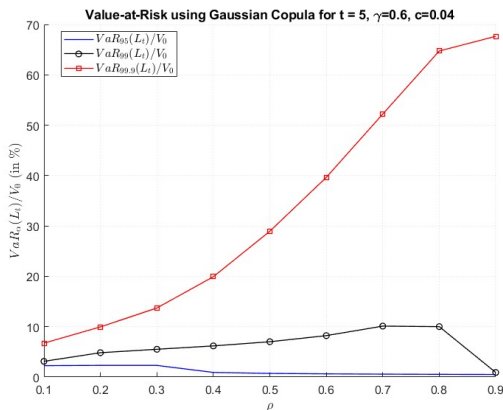
Comparing Figure 5a and 5b, we see that VaR increases as the correlation parameter rises. This is intuitive, as a higher correlation raises the probability of clusters of defaults. Focusing on the higher confidence levels (the tails), we observe that, for instance, at the 99.9% confidence level, the VaR rises to approximately 90% of the initial value, compared to below 45% in the lower correlation case. Again, our results in 5 are similar to those in Figure 9 in Herbertsson (2025a).

When ρ is increased further to 0.9, an extremely high correlation, the VaR changes drastically compared to Figures 5a and 5b. In Figure 5c, the VaR displays a more "all-or-nothing" behavior, where either almost all firms default or very few do. At the 99% confidence level, we observe an intermediate scenario where a sharp transition occurs around $t = 8$, and the VaR jumps from very low levels to above 90%. At the 99.9% confidence level, the extremely high correlation results in a VaR close to 100%, implying that if one firm defaults, the others are highly likely to follow due to the strong dependence. This behavior is consistent with stress scenarios, where correlations effectively increase as defaults occur, amplifying systemic risk and making extreme joint losses more likely.

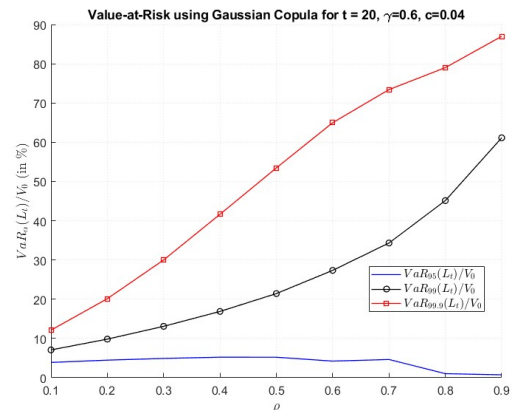
To illustrate the discrepancy between modeling defaults as discrete events and using a continuous asset pricing model, i.e. Black-Scholes model, we plot the relative difference between the VaR estimated under the Gaussian copula framework and the VaR implied by the Black-Scholes model in Figure 5d. The results in Figure 5d show that the one-factor Gaussian copula approach consistently produces significantly higher VaR estimates. This difference becomes more pronounced as the time horizon t increases, and it is further amplified at higher confidence levels. For instance, at the 99.9% confidence level, the relative difference in VaR starts at over 900% for short time horizons and rises to approximately 1400% as t increases. This under-

scores how discrete default modeling under a dependence structure such as the Gaussian copula can lead to substantially more conservative risk estimates compared to continuous models like Black-Scholes.

Next, we extend our analysis to a portfolio comprising of both stocks and bonds, modeled using the one-factor Gaussian copula. We consider a portfolio configuration with $\gamma = 0.6$, corresponding to 60% stocks and 40% bonds. To examine the impact of correlation on tail risk, we compute the VaR at confidence levels of 95%, 99%, and 99.9%, fixing the time horizon at $t = 5$ and $t = 20$ days while varying the correlation parameter, ρ , and holding all other parameters constant.



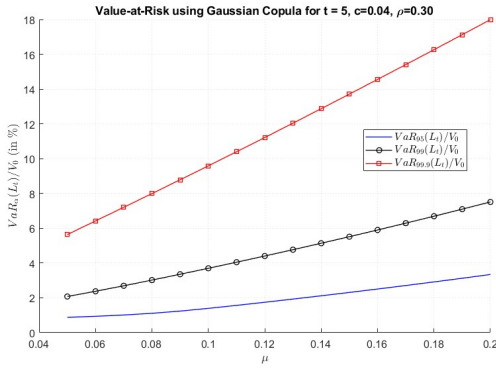
(a) $t = 5$ days



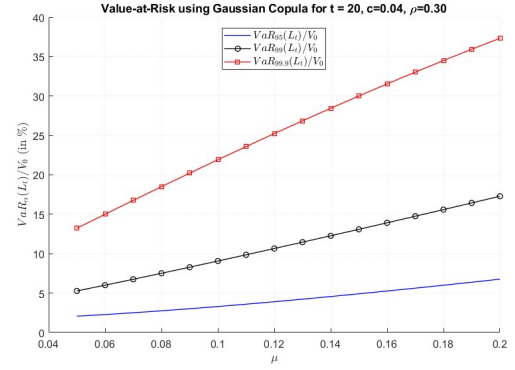
(b) $t = 20$ days

Figure 6: Value-at-Risk (in % of V_0) as function of Gaussian copula correlation parameter ρ at fixed time point $t = 5$ and $t = 20$ days for a portfolio with $\gamma = 0.6$, i.e. 60% stocks.

Figure 6 reveals distinct patterns in VaR evolution as ρ increases, particularly at high correlation level ($\rho \geq 0.8$). For $t = 5$, VaR at the 99% confidence level increases steadily with ρ but exhibits a sharp decline beyond a critical threshold ($\rho \geq 0.8$). This could be explained by the fact that a higher Gaussian correlation parameter ρ indicates heavier tails in the loss distributions. In contrast, for $t = 20$, VaR at higher confidence levels (99% and 99.9%) does not decline for higher levels of ρ . However, $VaR_{95\%}$ starts to decrease with ρ for when $\rho \geq 0.5$. This pattern indicates a persistent tail risk under extreme dependence over longer horizons.



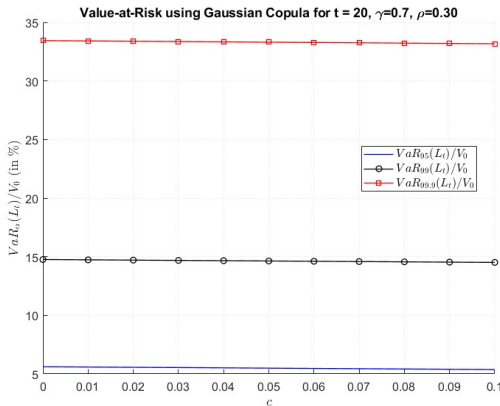
(a) $t = 5$ days



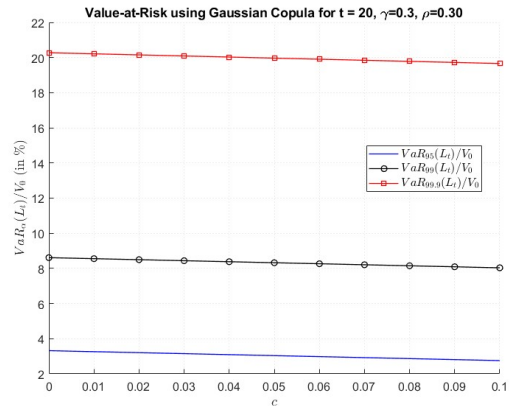
(b) $t = 20$ days

Figure 7: Value-at-Risk (in % of V_0) as function of μ at fixed time point $t = 5$ and $t = 20$ days for a portfolio with $\gamma = 0.6$.

Continuing our analysis, we investigate the effect of varying the drift parameter, μ , on the VaR for the credit portfolio consisting of 60% stocks and 40% bonds. Again, we fix the time horizons at $t = 5$ days and $t = 20$ days, and compute VaR for given confidence levels while varying μ . Figure 7 illustrates the resulting VaR profiles for both time horizons. Across all confidence levels, the VaR exhibits a steady increase with μ , following a similar pattern for $t = 5$ and $t = 20$.



(a) $\gamma = 0.7$



(b) $\gamma = 0.3$

Figure 8: Value-at-Risk (in % of V_0) as function of c at fixed time point $t = 20$ days for a portfolio with $\gamma = 0.7$ and $\gamma = 0.3$.

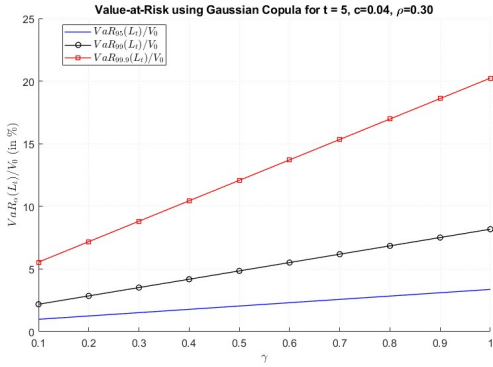
In Figure 8, we analyze the effect of varying the coupon rate (c) on the VaR. We consider two portfolio configurations, one with $\gamma = 0.7$ (70% stocks, 30% bonds) and another with $\gamma = 0.3$ (30% stocks, 70% bonds). We fix the time horizon at time $t = 20$ days. The VaR is significantly

lower for $\gamma = 0.3$ compared to $\gamma = 0.7$, reflecting the higher bond allocation’s stabilizing effect. Changes in c produce modest VaR shifts in both portfolios, with a more pronounced effect for $\gamma = 0.3$, consistent with its greater bond exposure, as bonds are directly influenced by the coupon rate. The modest effect of increasing the coupon rate is explained by the short time horizon.

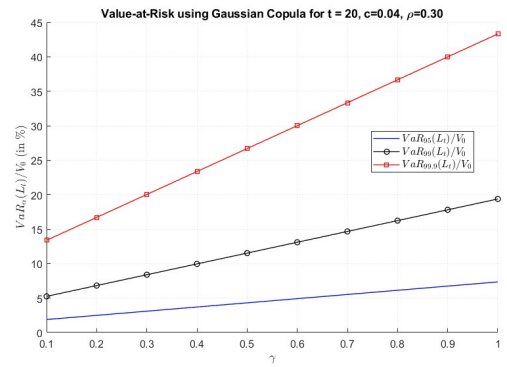
		$\gamma = 0.3$	$\gamma = 0.5$	$\gamma = 0.7$	$\gamma = 1$
$\rho = 0.3$	VaR 95%	1.51	2.04	2.57	3.37
	VaR 99%	3.52	4.85	6.18	8.18
	VaR 99.9%	8.81	12.08	15.34	20.24
$\rho = 0.6$	VaR 95%	0.28	0.51	0.75	1.11
	VaR 99%	4.87	7.11	9.34	12.69
	VaR 99.9%	24.97	34.75	44.52	59.18
$\rho = 0.9$	VaR 95%	0.22	0.41	0.61	0.90
	VaR 99%	0.42	0.75	1.08	1.58
	VaR 99.9%	40.58	57.55	74.53	100.00

Table 4: Value-at-Risk (in % of V_0) across different γ and ρ levels

Table 4 reports the VaR for various combinations of portfolio allocations and the default correlation parameter, evaluated at the 95%, 99%, and 99.9% confidence levels. We find that VaR increases monotonically with both γ and ρ , reflecting the compounding effect of higher exposure to stocks and stronger dependence among defaults. The increase in VaR is especially pronounced at higher confidence levels, most notably at the 99.9% level. Under high ρ , defaults are more likely to cluster, and when combined with large γ , the resulting VaR is amplified significantly. Since high quantile levels are sensitive to such rare events, the VaR at 99.9% reflects the full magnitude of this systemic risk.



(a) $t = 5$



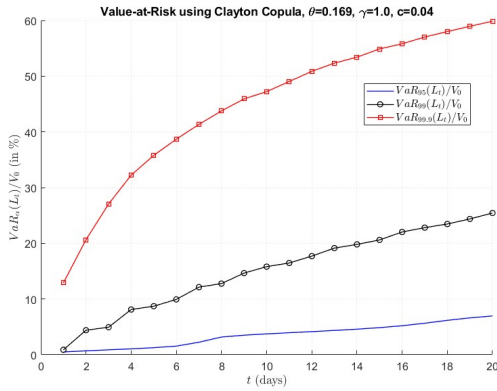
(b) $t = 20$

Figure 9: Value-at-Risk (in % of V_0) as function of γ at fixed time points $t = 5$ and 20 days and where $\rho = 0.3$.

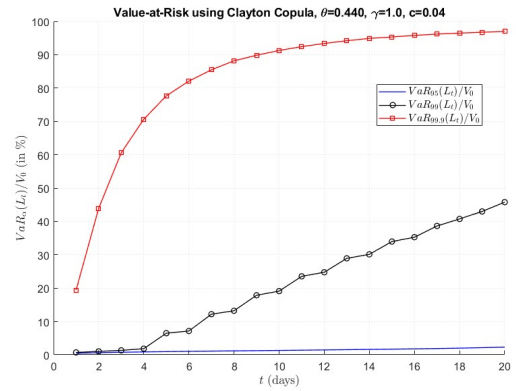
Figure 9 shows VaR as function of γ for $t = 5$ and $t = 20$. This could be interpreted as different portfolios, with the same parameters but with different compositions of stocks and bonds. As the stocks are generally more risky than bonds (have a higher probability of large losses), the VaR is higher for portfolios with greater exposure to stocks. For short time periods, such as 5 or 20 days, VaR becomes very high as the expected return of the stocks is relatively low. However, increasing the horizon could potentially lead to lower VaR estimates since the expected return could offset some of the downward jumps.

4.2.2 Value at Risk Estimation Using the Clayton Copula

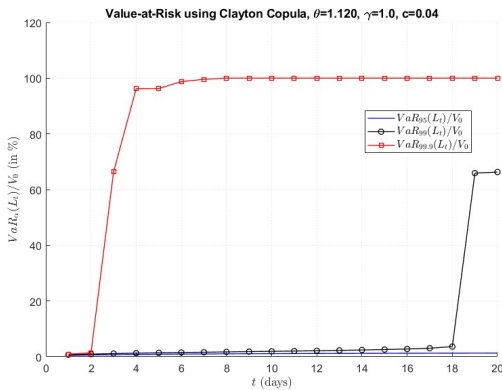
We now consider the Clayton copula model, using the same 20-day horizon as in the one-factor Gaussian copula model setup. Figures 10a to 10c illustrates the evolution of VaR, scaled by the initial portfolio value V_0 , for a portfolio consisting only of stocks, $\gamma = 1$, and Figure 10d shows the relative difference between the values in Figure 10a and the VaR from Black and Scholes (1973) model. We use three different dependence parameters, $\theta = 0.169$, which corresponds to a Gaussian copula with $\rho = 0.3$, $\theta = 0.44$, which matches $\rho = 0.6$, and $\theta = 1.12$ for $\rho = 0.9$. VaR is expressed as a percentage of the initial portfolio value V_0 . Furthermore, the VaR values are estimated using the parameters from Table 3. In general, the behavior in Figure 10 is similar to the one-factor Gaussian case in Figure 5.



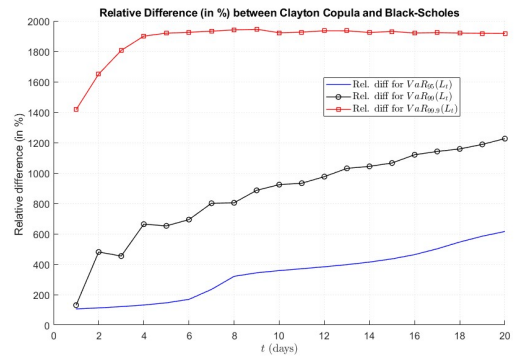
(a) $\theta = 0.169$



(b) $\theta = 0.44$



(c) $\theta = 1.12$



(d) Relative difference between VaR from Herbertsson (2025b) model for $\theta = 0.169$ and Black and Scholes (1973) model (in %).

Figure 10: Comparison of Value-at-Risk (in % of V_0) for different values of θ and the relative difference between VaR from Herbertsson (2025b) model and Black and Scholes (1973) model (in % of Black-Scholes VaR).

In Figure 10a, corresponding to $\theta_1 = 0.169$, the dependence between defaults is relatively weak, though still exhibiting some lower tail dependence. As a result, the increase in VaR across the given confidence intervals is present but remains comparatively moderate. The 99.9% VaR rises more sharply than the lower confidence levels, but its growth remains smooth and gradual over time. This indicates that while the model accounts for rare, large joint losses, it doesn't expect them to occur suddenly or with overwhelming intensity under this moderate dependence scenario. As time progresses, the gap between the 99.9% and 99% in Figure 10a VaR becomes noticeably larger than the gap between the 99% and 95% levels. This highlights how the Clayton copula, even with moderate dependence, places increasing weight on extreme joint losses at higher confidence levels.

Figure 10b, with $\theta_2 = 0.44$, illustrates how increased tail dependence drives a significant rise in extreme loss estimates, particularly at high confidence levels. Here, stronger lower tail dependence results in the 99.9% VaR escalating more rapidly, approaching 90% of the portfolio value for even small values of t . The 99% VaR also rises more steeply compared to Figure 10a, confirming that stronger dependence among defaults not only increases the likelihood of joint tail events but also accelerates the potential loss realization over short horizons. Interestingly, the 95% VaR remains relatively insensitive to the increase in θ , which suggests that this confidence level is less sensitive to stronger tail dependence.

Increasing the tail dependence further to $\theta = 1.12$ leads to even more abrupt changes in the time evolution of VaR, as illustrated in Figure 10c. For the highest studied confidence level, 99.9%, we observe a sharp increase in VaR early on (i.e., for small t), indicating that this risk measure is extremely sensitive to rare, extreme events. Although such events are unlikely, their potential impact is significant. At the 99% confidence level, a similar sharp increase occurs, but at a later stage (larger t).

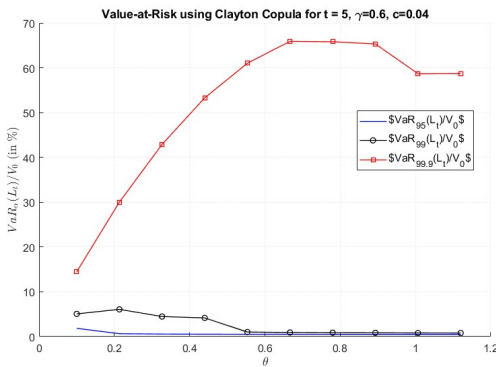
The relative difference between the VaR estimated using the Clayton copula and the Black-Scholes VaR is shown in Figure 10d. Similarly to the relative difference between Gaussian VaR and Black-Scholes, the Clayton VaR is significantly higher than the Black-Scholes VaR. Most prominently for $\text{VaR}_{99.9\%}$, where it peaks at almost 20 times higher VaR than the Black-Scholes, but also for lower confidence levels. While the relative difference for $\text{VaR}_{95\%}$ and $\text{VaR}_{99\%}$ increases consistently after $t = 4$, we see that the relative difference for $\text{VaR}_{99.9\%}$ remains relatively steady after this point.

The time evolution of VaR under the one-factor Gaussian copula and the Clayton copula reveals notable differences, particularly at higher confidence levels. As shown earlier, the VaR estimates derived from the Clayton copula framework are consistently higher than those from the Gaussian copula, even when the dependence parameters are calibrated to yield comparable average correlations.

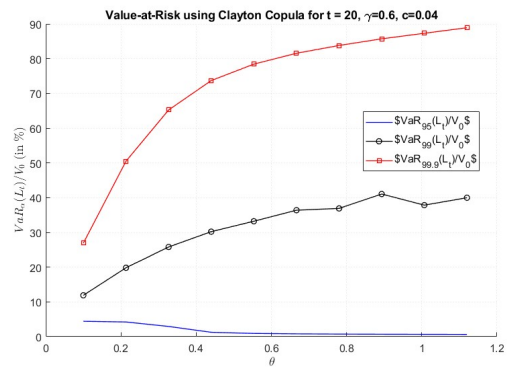
For example, comparing the Gaussian copula with $\rho = 0.3$, Figure 5a, to the Clayton copula with $\theta = 0.169$, Figure 10a, we observe that at the 99.9% confidence level, the VaR under the Clayton copula reaches approximately 60% of the initial value of the portfolio, while the Gaussian copula model yields only about 45%. A similar pattern holds when ρ is increased to 0.6 and compared

to a Clayton copula with $\theta = 0.44$, where the Clayton-based VaR climbs to around 90% after just 10 days, whereas the Gaussian counterpart levels off closer to 75% over the same horizon. Increasing ρ to 0.9 under the Gaussian framework and comparing it to a Clayton copula with $\theta = 1.12$ reveals similar overall patterns, but also some notable differences. Under the Gaussian framework, the Value-at-Risk (VaR) at the 99.9% confidence level reaches nearly 100% almost immediately. In contrast, the Clayton copula exhibits a delayed but abrupt increase in VaR after a short time, although still at an early stage (small t). At the 99% confidence level, both models display a sharp increase in VaR, transitioning from very low to nearly 100% over a short time horizon. However, the Clayton copula shows this behavior significantly later compared to the Gaussian model. For the 95% confidence level, the two models produce nearly identical results, with VaR remaining flat at low levels across the time horizon. This suggests that VaR is relatively insensitive to extreme dependence structures at lower confidence levels.

These differences are a direct consequence of the structural properties of the two copulas. The one-factor Gaussian copula assumes symmetric dependence and lacks tail dependence, which leads to an underestimation of joint extreme events. In contrast, the Clayton copula exhibits strong lower tail dependence, making it more sensitive to clustered defaults and extreme co-movements in the lower tail of the distribution. This property leads to a steeper increase in VaR for higher quantiles and longer horizons, making the Clayton copula particularly suitable for stress testing and risk assessment in scenarios involving joint credit events or systemic shocks.



(a) $t = 5$ days



(b) $t = 20$ days

Figure 11: Value-at-Risk (in % of V_0) as function of Clayton copula parameter θ at fixed time point $t = 5$ and $t = 20$ days for a portfolio with $\gamma = 0.6$.

In Figure 11, we examine the impact of varying the dependence parameter θ on the estimated VaR. For a time horizon of $t = 5$, both $\text{VaR}_{95\%}$ and $\text{VaR}_{99\%}$ decrease as θ increases, while $\text{VaR}_{99.9\%}$ initially increases for $\theta \leq 0.68$, and then begins to decrease for higher values of θ . As the dependence parameter reaches very high levels, the VaR estimates begin to exhibit a different pattern, characterized by a flattening trend followed by a slight decline. When extending the time horizon to 20 days, a similar trend emerges. Both $\text{VaR}_{99\%}$ and $\text{VaR}_{99.9\%}$ increase with higher θ , while $\text{VaR}_{95\%}$ remains very low and continues to decrease toward zero as θ increases.

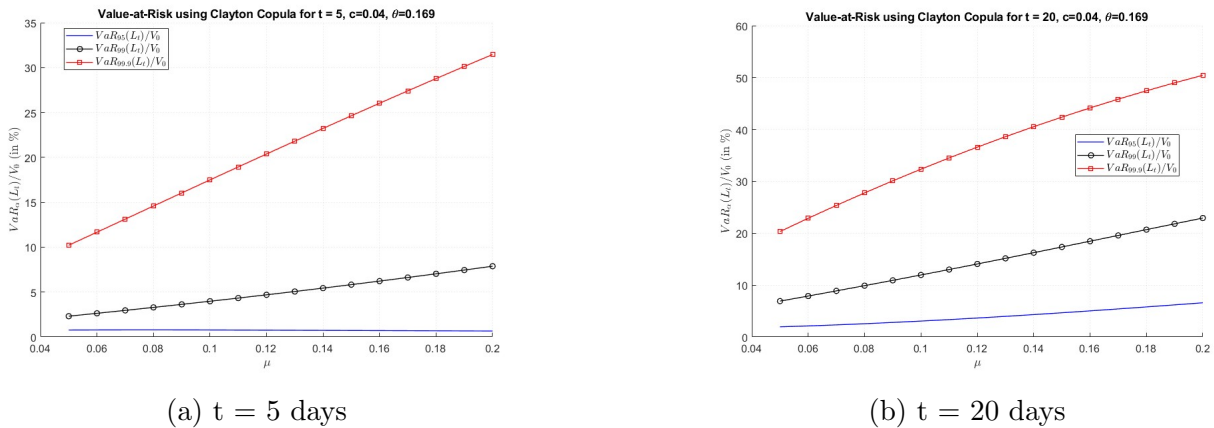


Figure 12: Value-at-Risk (in % of V_0) as function of μ at fixed time point $t = 5$ and $t = 20$ days and where $\theta = 0.169$ for a portfolio with $\gamma = 0.6$.

Figure 12 examines how VaR behaves as a function of the drift parameter μ under a Clayton copula with $\theta = 0.169$ and $\gamma = 0.6$. Results are shown for two fixed time horizons, $t = 5$ (Figure 12a), and $t = 20$ (Figure 12b). At both time horizons, increasing μ leads to a consistent upward shift in all VaR estimates, as a higher average loss rate naturally implies greater risk. This effect is most pronounced at the 99.9% level, which exhibits the steepest rise across the entire range of μ .

While the general upward trend is present in both Figure 12a and Figure 12b, a key distinction emerges at the longer horizon, $t = 20$, where the rate at which VaR increases begins to diminish gradually for higher μ . This flattening, most noticeable in the 99.9% VaR curve, suggests a diminishing sensitivity of tail risk to further increases in drift. The shape of the VaR curves remains relatively stable between the two time frames, with no sudden nonlinearities. This indicates that while time horizon magnifies overall risk levels, it does not fundamentally alter

the way μ interacts with the loss distribution under the current model settings.

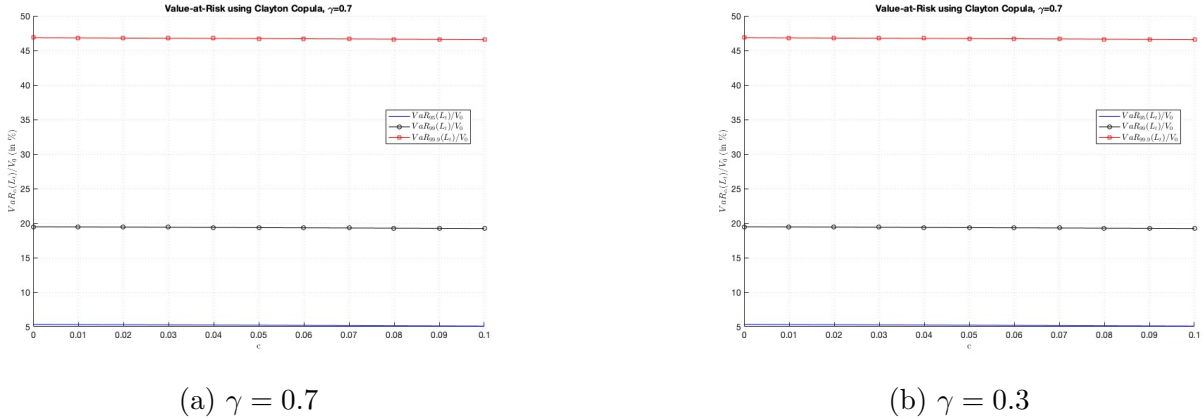


Figure 13: Value-at-Risk (in % of V_0) as function of c at fixed time point $t = 20$ days and where $\theta = 0.169$ for a portfolio with $\gamma = 0.7$ and $\gamma = 0.3$.

Figure 13 shows how the VaR responds to variations in the bond coupon rate, c . The analysis is conducted at a fixed time horizon of 20 days, with the dependence parameter set to $\theta = 0.169$. Two portfolio allocations are considered, one consisting of 70% stocks and 30% bonds ($\gamma = 0.7$), and the reverse allocation of 30% stocks and 70% bonds ($\gamma = 0.3$). In both cases, the coupon rate varies from 0 to 0.1.

Across all confidence levels and both portfolio allocations, the VaR curves remain almost flat as c increases. This outcome holds regardless of whether the portfolio is tilted towards stocks or bonds, suggesting that short-term credit risk, as captured in this 20-day horizon, is largely unaffected by changes in bond yield. The limited sensitivity likely stems from the short time horizon, during which coupon rates have only a marginal impact on the overall loss distribution, especially when compared to factors like default correlation, θ , or the drift parameter, μ .

		$\gamma = 0.3$	$\gamma = 0.5$	$\gamma = 0.7$	$\gamma = 1$
$\theta = 0.169$	VaR 95%	0.32	0.59	0.85	1.26
	VaR 99%	3.67	5.11	6.55	8.70
	VaR 99.9%	16.27	21.85	27.42	35.78
$\theta = 0.44$	VaR 95%	0.23	0.43	0.64	0.94
	VaR 99%	2.45	3.60	4.75	6.47
	VaR 99.9%	34.99	47.18	59.37	77.66
$\theta = 1.12$	VaR 95%	0.21	0.40	0.59	0.87
	VaR 99%	0.36	0.65	0.95	1.39
	VaR 99.9%	30.50	49.29	68.08	96.26

Table 5: Value-at-Risk (in % of V_0) across different γ and θ levels

Table 5 presents the VaR estimates at three confidence levels (95%, 99%, and 99.9%) for different combinations of portfolio allocation, γ , and dependence structure parameter, θ , in the Clayton copula. As expected, VaR increases with the confidence level, reflecting greater sensitivity to extreme tail events. Additionally, VaR rises as the portfolio becomes more equity-heavy, i.e., as γ increases from 0.3 to 1.

The Clayton copula, known for its ability to model lower tail dependence, captures extreme co-movements more effectively than the one-factor Gaussian copula. Consequently, VaR estimates in Table 5 are generally higher at the 99.9% level compared to those reported in Table 4, where the Gaussian copula is used. This difference is particularly pronounced at higher dependence levels, which are matched across tables using comparable parameter pairs, where $\rho = 0.3$ corresponds to $\theta = 0.169$, $\rho = 0.6$ to $\theta = 0.44$, and $\rho = 0.9$ to $\theta = 1.12$.

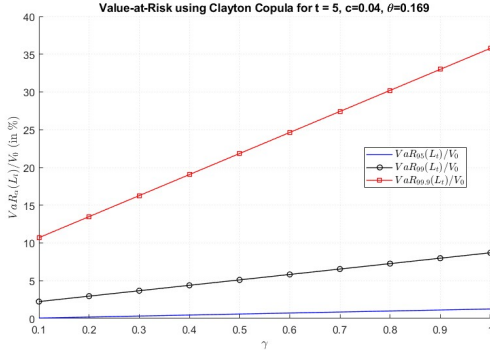
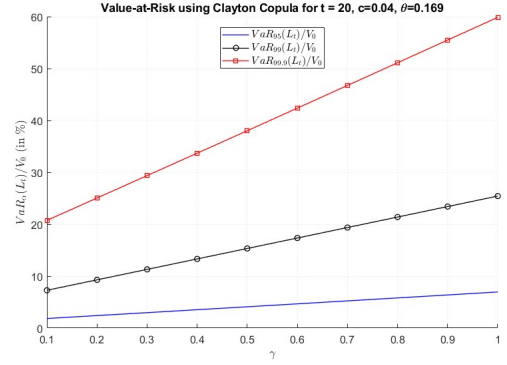
(a) $t = 5$ (b) $t = 20$

Figure 14: Value-at-Risk (in % of V_0) as function of γ at fixed time points $t = 5$ and 20 days and where $\theta = 0.169$.

Similarly to the Gaussian case in Figure 9, in Figure 14 we observe that portfolios with a larger stock allocation γ exhibit higher VaR levels, both over the 5-day and 20-day horizons. This outcome is intuitive and aligns with standard financial theory, as equities generally carry higher volatility and greater exposure to jump risk than bonds. Notably, the relationship between VaR and the portfolio's stock allocation appears approximately linear, suggesting that risk increases proportionally with equity exposure, at least within the observed short-term time frames. During these short time intervals, it is likely that the time is too short for the compounding effects of drift or coupon accumulation to significantly impact the portfolio value. Moreover, the fact that this pattern holds under both the Gaussian and Clayton copulas despite their differing dependence structures indicates a certain robustness in the relationship between VaR and equity allocation.

5 Conclusion

In this thesis, we studied the risk characteristics of portfolios composed of both equities and defaultable bonds, focusing on the compounding effect of bond defaults triggering downward jumps in stock prices. By comparing the model introduced by Herbertsson (2025b) to the classical Black and Scholes (1973) model, we show that neglecting jump risk and default clustering can lead to a dramatic underestimation of potential losses. The VaR estimates derived under Herbertsson's model were consistently and substantially higher, particularly at high confidence levels and over short horizons, often exceeding the Black-Scholes estimates by more than

1000%.

An important aspect of the analysis is the comparison between the one-factor Gaussian and Clayton copulas, which were used to model default dependence. The results indicate that while both structures lead to higher VaR estimates as correlation increases, the Clayton copula, due to its lower tail dependence, produces more conservative risk estimates, particularly at high confidence levels. This effect is most pronounced at extreme quantiles, where the likelihood of clustered defaults increases.

Beyond dependence modeling, the analysis highlights how portfolio composition, asset dependence, drift, and the coupon rate influence downside risk. Increasing the equity share consistently raises VaR, as a higher stock allocation increases the portfolio's exposure to jump risk triggered by bond defaults. Similarly, stronger asset dependence, modeled through higher copula parameters, amplifies the likelihood of clustered defaults, resulting in more severe losses.

Overall, the findings underline the importance of incorporating default-driven jumps and realistic dependence structures when assessing the downside risk of stock–bond portfolios, particularly in environments where credit stress and contagion effects are relevant.

Future work could extend the present analysis by applying the model introduced by Herberets-son (2025b) to real-world market data, enabling empirical validation and potentially uncovering further insights into jump risk and default clustering under observed credit conditions. Such an extension would not only enhance the model's practical relevance but also open up discussions around model calibration, parameter stability, and predictive accuracy. Another promising direction is to apply the model within a portfolio optimization framework, where the objective is to minimize VaR with respect to the portfolio allocation. This approach could help identify optimal stock–bond allocations under credit risk, thereby bridging the gap between risk quantification and actionable investment strategy.

References

- Andersson, F., Mausser, H., Rosen, D., & Uryasev, S. (2001). Credit Risk Optimization with Conditional Value-at-Risk criterion. *Mathematical Programming*, 89(2), 273–291.
- Artzner, P., Delbaen, F., Eber, J.-M., & Heath, D. (1999). Coherent Measures of Risk. *Mathematical Finance*, 9(3), 203–228.
- Bates, D. S. (1996). Jumps and Stochastic Volatility: Exchange Rate Processes Implicit in Deutsche Mark Options. *The Review of Financial Studies*, 9(1), 69–107.
- Bates, D. S. (2000). Post-'87 crash fears in the SP 500 futures option market. *Journal of Econometrics*, 94(1-2), 181–238.
- Black, F., & Scholes, M. (1973). The pricing of options and corporate liabilities. *Journal of Political Economy*, 81(3), 637–657.
- Brown, P. J. (2006). *An introduction to the bond markets*. wiley.
- Burtschell, X., Gregory, J., & Laurent, J. (2009). A comparative analysis of CDO pricing models under the factor copula framework. *Journal of Derivatives*, 16, 9–37.
- Cairns, A. J. G. (2004). *Interest rate models: An introduction*. Princeton University Press.
- Carr, P., & Wu, L. (2003). What Type of Process Underlies Options? A Simple Robust Test. *The Journal of Financial*, 58(6), 2581–2610.
- Chen, N., & Kou, S. G. (2009). Credit spreads, optimal capital structure, and implied volatility with endogenous default and jump risk. *Mathematical Finance*, 19(3), 343–378.
- Chernov, M., Gallant, A. R., Ghysels, E., & Tauchen, G. (2003). Alternative models for stock price dynamics. *Journal of Econometrics*, 116(1-2), 225–257.
- Das, S. R., Duffie, D., Kapadia, N., & Saita, L. (2007). Common Failings: How Corporate Defaults are Correlated. *Journal of Finance*, 62(1), 93–117.
- Duffie, D., & Pan, J. (1997). An Overview of Value at Risk. *Preliminary Draft*.
- Eraker, B. (2004). *Do Stock Prices and Volatility Jump? Reconciling Evidence from Spot and Option Prices*.
- Geman, H., Madan, D. B., & Yor, M. (2001). Time Changes for Lévy Processes. *Mathematical Finance*, 11(1), 79–96.
- Gourieroux, C., Laurent, J., & Scaillet, O. (2000). Sensitivity analysis of Values at Risk. *Journal of Empirical Finance*, 7(3-4), 225–245.

- Grootveld, H., & Hallerbach, W. (1999). Variance vs downside risk: Is there really that much difference? *European Journal of Operational Research*, *114*(2), 304–319.
- Guerrera, F., Guha, K., & Farrell, G. (2008). Wall Street crisis hits stocks [Available at: <https://on.ft.com/42x9aKP> (Accessed: April 5th, 2025)]. *Financial Times*.
- Herbertsson, A. (2023). Saddlepoint Approximations for Credit Portfolio Distribution with Applications in Equity Risk Management [Working paper].
- Herbertsson, A. (2025a). Risk Management of Stock Portfolios with Jumps at Exogeneous Default Events. *Frontiers of Mathematical Finance*, *4*, 25–101.
- Herbertsson, A. (2025b). Value-at-Risk and Expected Shortfall for Stock-Bond Portfolios with Downward Jumps in Stocks at Default of the Bonds [Working paper, forthcoming on SSRN].
- Hofert, M., & Scherer, M. (2011). CDO pricing with nested archimedean copulas. *Quantitative Finance*, *11*, 775–787.
- Johnson, M. A., & Mamun, A. (2012). The failure of Lehman Brothers and its impact on other financial institutions. *Applied Financial Economics*, *22*, 375–385.
- Kole, E., Koedijk, K., & Verbeek, M. (2007). Selecting Copulas for Risk Management. *Journal of Banking and Finance*, *31*, 2405–2423.
- Kou, S. G. (2002). A jump-diffusion model for option pricing. *Management Science*, *48*(8), 1086–1101.
- Li, D. X. (2000). On Default Correlation: A Copula Function Approach. *The Journal of Fixed Income*, *9*, 43–54.
- Malevergne, Y., & Sornette, D. (2003). Testing the Gaussian copula hypothesis for financial assets dependences. *Quantitative Finance*, *3*(4), 231–250.
- Merton, R. C. (1976). Option pricing when underlying stock returns are discontinuous. *Journal of Financial Economics*, *3*(1-2), 125–144.
- Patton, A. J. (2012). A review of copula models for economic time series. *Journal of Multivariate Analysis*, *110*, 4–18.
- Zhou, C. (2001). The term structure of credit spreads with jump risk. *Journal of Banking & Finance*, *25*(11), 2015–2040.